Master Thesis

# The Effect of Ultrasonic Excitation on Ice as a Substitute for Natural Gas Hydrates

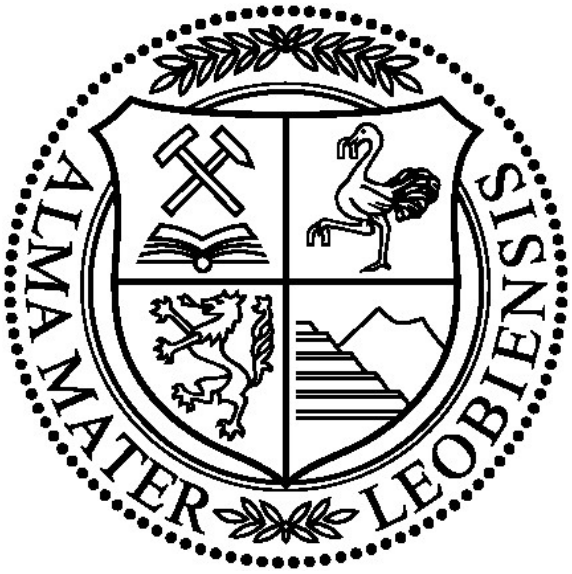


**Written by:**
Philipp A. Zellnig, BSc
00835167

**Advisor:**
Univ.-Prof. Dipl.-Ing. Dr.mont. Herbert Hofstätter
Dipl.-Ing. Mikhail Pavlov

Leoben, 02. September 2018

# EIDESSTATTLICHE ERKLÄRUNG

Ich erkläre an Eides statt, dass ich die vorliegende Diplomarbeit selbständig und ohne fremde Hilfe verfasst, andere als die angegebenen Quellen und Hilfsmittel nicht benutzt und die den benutzten Quellen wörtlich und inhaltlich entnommenen Stellen als solche erkenntlich gemacht habe.

Leoben, 02. September 2018
Ort, Datum

Philipp Zellnig

# AFFIDAVIT

I hereby declare that the content of this work is my own composition and has not been submitted previously for any higher degree. All extracts have been distinguished using quoted references and all information sources have been acknowledged.

Leoben, September 02, 2018
Place, Date

Philipp Zellnig

# Acknowledgements

First of all, I want to thank my supervisor Dipl.-Ing. Mikhail Pavlov for offering me this study, for his excellent guiding, and for supporting me during my work on this thesis. All the discussions, his vast knowledge and good ideas motivated me a lot to complete my scientific work.

Furthermore, I want to thank the Head of Chair of Petroleum and Geothermal Energy Recovery Univ.-Prof. Dipl.-Ing. Dr.mont. Herbert Hofstätter for his supervision throughout my entire master program. I appreciate him as great teacher and mentor in all practical and theoretical aspects.

Special acknowledgments go to my family, particularly my parents, grandmother and my sister, who always supported me in all matters, my father, without whom I wouldn't have been able to finish my studies, to Eva-Maria, for being the best partner and friend I can ever wish for and finally to all my friends, who encouraged me during my whole study at the Montanuniversität Leoben.

# Kurzfassung

Neueste Erkenntnisse durch Feld- und Laborversuche haben in den letzten Jahren gezeigt, dass die Anwendungen von Ultraschall in der Erdöl- und Erdgasindustrie vielseitig und in den meisten Fällen nicht nur aus technischer Sichtweise Sinn machen, sondern auch eine wirtschaftliche, nachhaltige und effiziente Alternative zu heute gängigen Methoden darstellen.

Die Grundzüge dieser Arbeit konzentrieren sich einerseits auf die verschiedenen Anwendungsbereiche von Ultraschall in der Erdöl- und Erdgasindustrie und legt andererseits ihren Fokus auf die Auswirkungen von Ultraschallwellen auf Eis, welches als Stellvertreter für Gashydrate angesehen werden kann. Im direkten Zusammenhang wird eine sichere, effiziente und umweltfreundliche Methode gesucht um solche Gashydrate mit Ultraschall entfernen zu können. Die Bildung von Gashydraten während der Produktion, der Verarbeitung und dem Transport von Erdgas stellt ein großes Problem dar. Vorfälle, die direkt oder indirekt mit der Handhabung von Gashydraten zusammenhängen, kosten der Erdgasindustrie Millionen von Dollar. Viel schlimmer ist die Bedrohung von Menschenleben durch Unfälle oder unsachgemäßes Verhalten. Daher ist das Verständnis für eine effektive Hydratprävention und in weiterer Folge für die Entfernung von Hydratablagerungen und Verstopfungen ein entscheidender Faktor, der eine ständige Entwicklung und Verbesserung fordert.

Um die Wirkung von Ultraschall auf Eis bewerten zu können, werden drei unterschiedliche Experimente durchgeführt. Zur ersten Orientierung (Setup 1) wird ein einfacher Ultraschallreiniger, der üblicherweise im Haushalt Anwendung findet, eingesetzt. Ein sofortiger Effekt des Ultraschalls ist sowohl visuell als auch akustisch wahrnehmbar: in unterschiedlichen Bereichen des Eisblocks treten Luftblasen auf, die auf den Effekt der Kavitation zurückzuführen sind. In weiterer Folge bricht das Eis und es entstehen flüssigkeitsgefüllte Hohlräume. Im Vergleich zum Kontrollexperiment unter normalen Bedingungen ohne Ultraschall wird eine 24-mal schnellere Auflösung beobachtet. Der zweite Versuchsaufbau (Setup 2) setzt sich mit dem Zerfall, beziehungsweise der Zerstörung, von Hydratstopfen in einem Stahlzylinder, der einen Rohrabschnitt darstellt, auseinander. Die Ultraschallanregung beweist hierbei eine um eine vielfache schnellere Auflösung, außerdem können Veränderungen der mechanischen Eigenschaften des Eises beobachtet werden: der Eisblock wird brüchig, instabil und zerfällt unter leichtester Beanspruchung. Der Schwerpunkt der Arbeit liegt jedoch auf Setup 3, da hierbei durch das Anlegen eines Kontrolldruckes an den Einlass des Zylinders, Auskunft über den Durchbruch des Eisblocks gegeben werden kann. Dieser Punkt ist wesentlich, da er verdeutlicht, ab wann eine Druck- oder Strömungskommunikation zwischen dem Einlass und dem Auslass gegeben ist und somit den Zeitpunkt darstellt, ab wann ein verstopftes Rohr wieder „frei“ fließen kann.

Generell können bei allen Versuchen unter Ultraschallanregung schnellere Zerfall- und Durchbruchzeiten beobachtet werden. Untersuchungen bezüglich unterschiedlich starker

Ultraschallsignale, realisiert durch die unterschiedliche Anzahl an Ultraschallwandlern mit Gesamtleistungen von 200, 400 oder 1000 Watt zeigen nicht notwendigerweise eine Verbesserung der Anwendung. Zusammengefasst, ein Anstieg der Leistung bedeutet keinesfalls einen Anstieg der Auflösungseffizienz.

Alle Experimente dieser Arbeit vergleichen die Wirkung von Ultraschall mit den Ergebnissen von nicht beschallten System bei Umgebungsbedingungen. Um industriell relevante Vergleiche mit gängigen Methoden der Hydratentfernung zu erhalten, sind weitere wissenschaftliche Anstrengungen und Experimente notwendig.

# Abstract

In recent years, field tests and laboratory investigations have demonstrated that applications of ultrasound in the oil industry are versatile and in many cases not only technologically feasible, but also serve as an economical, sustainable and efficient alternative to currently accepted methods.

This thesis focuses on the understanding of ultrasonic treatment in different disciplines throughout the oil industry and especially gives insights of the behavior of ultrasonic waves on ice as a substitute for natural gas hydrates and further aims at their safe, efficient and environmentally friendly removal. The formation of hydrates is one of the problems occurring during production, processing and transportation of natural gas. Incidents directly or indirectly associated with hydrates and their mishandling cost the natural gas industry millions of dollars. Even worse is the threatening of human lives due to accidents or improper operations. Therefore, the inhibition of hydrate formation and the effective removal of hydrate precipitations and plugs are a crucial task to understand and prompt constant improvement.

Three different sets of experiments are performed to evaluate the effect of ultrasound on ice. For first orientation (Setup 1), a simple household ultrasonic cleaner with a basic setup is used. An instant effect is visually and acoustically perceptible after the ultrasonic signal is turned on. Small air bubbles emerge at certain spots inside the block of ice as a result of ultrasonic cavitation. Fractures and cavities are further results of the mechanical energy input. In the best case, the disintegration of the ice block was 24 times faster than under ambient conditions. Setup 2 compares the duration of ice plug removal in a prototype steel cylinder. A much faster disintegration of the ice plug is reached under ultrasonic excitation. Further, the mechanical properties of ice drastically change under ultrasound as the plug gets very brittle, instable and breaks easily. The main focus lies on Setup 3, as the steel cylinder is pressurized to get information about the temporal dissolution of the plug under pressure and the influence of changing ultrasonic fields. Pressure breakthrough times are evaluated in this set of experiments. The breakthrough time is a crucial parameter as it clarifies at which point a pressure or flow communication between an inlet and an outlet is granted. Therefore, it represents the time how long it takes until a plugged pipe can flow again. Further, different ultrasonic energy inputs are compared. Throughout all experiments under ultrasonic excitation faster disintegration of ice and decreasing breakthrough times are observed. In most cases an increase in energy does not necessarily mean a higher efficiency of disintegration, which approximately remains constant as long as any ultrasonic signal is applied.

All experiments in this thesis investigate the effect of ultrasound compared to a non-sonicated system at ambient conditions. Further comparison to other common removal methods require additional experiments.

# List of Tables

# List of Figures

# Abbreviations

| | |
|---|---|
| US | Ultrasound |
| NUS | Non-ultrasound |
| SEM | Scanning electron microscope |
| SL | Sonoluminescence |
| SPF | Surfactant polymer flooding |
| IFT | Interfacial tension |
| CMC | Critical micelle concentration |
| OOIP | Original oil in place |
| UR | Ultimate recovery |
| BP | Breakpoint |
| CT | Computerized Tomography |
| k | thousand |
| M | million |

# Table of content

Page

# 1 Introduction

The world oil resources are limited and the exploitation of oil fields to a higher degree is desirable, thus new methods are required to improve the recovery rates of oil fields and to recover most of the oil found in pores. Difficulties arise during the excessive production of oil or gas from underground reservoirs, as chemical and mechanical processes can affect the wellbore. Many of these processes can eventually cause a problem with the well, resulting either in a decrease in production or in failure of equipment installed downhole or at the surface. Therefore, great effort is being made to increase the overall efficiency of production systems and reduce the meantime between failure to keep shut downs at a minimum. This is best achieved by understanding critical processes and finding new technologies to combat occurring problems. [1]

In recent years, field tests and laboratory investigations have demonstrated that applications of ultrasound in the oil industry are versatile and range from enhanced oil recovery (EOR) to well stimulation, wellbore cleaning, and soil remediation. Recent studies even show a possibility to alter fluid properties and prevent crystallization and precipitation of heavier components. Ultrasound as a well-known technology is in many cases not only technologically feasible, but also serves as an economical, environmentally friendly and efficient alternative to currently accepted methods. Therefore, further scientific effort needs to be directed into the development of new fields of application of ultrasound.

This thesis focuses on the understanding of ultrasonic treatment in different disciplines of the oil industry and especially gives insights of the behaviour of ultrasonic waves on ice as a substitute for natural gas hydrates and further aims at their safe, efficient and environmentally friendly removal. An important reason for understanding hydrate blockages is safety, as every few years a major injury or major equipment damage occurs, due to hydrates. [2]

## 1.1 Problem Definition

The formation of hydrates is one of the problems occurring during production, processing and transportation of natural gas. Incidents directly or indirectly associated with hydrates and their mishandling cost the natural gas industry millions of dollars. Even worse is the threatening of human lives due to accidents or improper operations. Therefore, the inhibition of hydrate formation and the effective removal of hydrate precipitations and plugs are a crucial task to understand and prompt constant improvement. [3]

Currently accepted methods for hydrate plug remediation although being effective can have some undesirable side effects. Used chemicals can be toxic, are cost intensive and if not removed properly can decrease the value of the produced fluid. Therefore, the transition to mechanical disintegration methods is desirable.

## 1.2 Objective

Consequently, this thesis aims to clarify the impact of ultrasound on ice as a substitute for natural gas hydrates to possibly find a new hydrate plug remediation method. Hereby, the focus lies on the mechanical disintegration of ice under different ultrasonic properties. More in detail, the dissolution of ice is studied as function of pressure conditions, ultrasonic energy input, resonant frequency and excitation time. Main influencing parameters on disintegration efficiency are investigated.

# 2 Fundamentals and Literature Review

## 2.1 Ultrasound

The following chapter deals with a review of methods and results of previously published works and studies investigating ultrasound stimulation of oil and gas wells. This review is organized thematically; starting with the theoretical basics of ultrasound and wave phenomena, heading to enhanced oil recovery where a drastic permeability increase is observed due to deformation of the wall of a pore, altering its radius and leading to fluid displacement similar to “peristaltic transport”. Further investigation is about the removal of plugging material from the wellbore and near-wellbore regions and discussing ultrasound cleaning in general. The last part covers the alteration of fluid properties as a part of preventative ultrasound treatment.

### 2.1.1 General

To be able to understand the mechanism and the real potential of ultrasound (US) stimulation of oil wells, it is crucial to have basic knowledge of the wave phenomenon, its properties, its behavior and its interaction with the propagation media. Caicedo in 2007 presented a paper that covers these basic ideas. [4]

For each ultrasound application (diagnosis, quality control, cleaning, stimulation, etc.) specific power and frequency ratings have to be considered. Further, the effect of the media on the propagation of the US wave needs to be examined and understood. US is a pressure wave created usually by piezoelectric or magnetostrictiv transducers with a frequency above 20 kHz. It propagates in a continuous media with elastic properties by means of deformation of the media’s particles parallel to the propagation axis and again returning to their original position. Pressure p(x,t) is a “P” wave and can be understood by applying basic physical definitions of period (T) and wave length (λ) to its harmonic solution **eq.1** [4, p. 3] and introducing the solution into the basic wave equation **eq.2** [4, p. 3]. The result is the very important dispersion relationship **eq.3** [4, p. 3], which links wavelength, velocity and frequency.

$$p(x,t) = p_0 \cos(kx - \omega t) \qquad (1)$$

$$(\alpha + 2\mu)\nabla^2 p = \rho \frac{\partial^2 p}{\partial t^2} \qquad (2)$$

$$\lambda = \frac{V}{f} \qquad (3)$$

Table 1 shows representative wavelength and frequency values for a velocity of 3000 m/s as this is the expected propagation velocity in rocks. Previous research from Venkitaraman and

Van der Bas [5] though made clear that an increase of frequency for better cleaning ability reduces the wavelength which decreases the stimulation effectivity. Further the attenuation effect has to be considered. By assuming friction, it is clear that a higher frequency leads to a higher attenuation, resulting in an increased loss of energy during propagation.

Table 1: Wavelength references [4, p. 3]

| | ***Exploration*** | ***Reference*** | | ***Treatments*** | | ***Diagnosis*** | |
|---|---|---|---|---|---|---|---|
| | Geophysics | Human ear | | Ultrasound | | Ultrasound | |
| | | min | max | min | max | min | max |
| *Velocity v [m/s]* | 3000 | 3000 | 3000 | 3000 | 3000 | 3000 | 3000 |
| *Frequency f [Hz]* | 60 | 20 | 19k | 20k | 100k | 1M | 10M |
| *Wavelength $\lambda$ [m]* | 50 | 150 | 0.16 | 0.15 | 0.03 | 0.003 | 0.0003 |

For source power requirements, also the propagation effect needs to be considered to guarantee sufficient power inside the formation. Most influencing factors are interphases and geometry. Differentiations have to be made in casedhole- and openhole- applications to allow a valid analysis for reflected and transmitted waves. In cased holes only 9% of the source energy is transmitted to the reservoir face, in openhole- completions energy yields a higher value of about 47%, respectively. The last phenomena to consider for energy and intensity estimations are interference and diffraction, which lead to superposition of ultrasonic waves. The result is destructive interference; that means in some points the signal is zero and no cleaning or stimulation effect can be observed. Finally, intensity and power ratings can be calculated by including all previously discussed effects with following equations. **eq.4** [4, p. 4]

$$I = \frac{Power_{RMS}}{A} = \frac{(\alpha+2\mu)}{\alpha+2\mu/3)}\frac{1}{2}\frac{p_0^2}{\rho V} \qquad (4)$$

Concerning a pipe with radial properties **eq.5** [4, p. 4]

$$I(r) = I_0 \frac{r_w}{r} \qquad (5)$$

and including friction **eq.6** [4, p. 4]

$$I(r) = I_0 \frac{r_w}{r} e^{-2\beta(\omega)k(r-r_w)} \qquad (6)$$

Considering interference and diffraction concludes into the final equation **eq.7** [4, p. 5].

$$I_{RMS} = E_0^2 cos^2(\frac{\pi dz}{\lambda L}) \frac{sen^2(\frac{\pi bz}{\lambda L})}{(\frac{\pi bz}{\lambda L})^2} \qquad (7)$$

Caicedo concludes his paper with a possible definition of an application window for ultrasound stimulation. He states that ultrasound is a mechanical phenomenon that should be applied for damages that can be removed mechanically:

- Removing of near wellbore damage due to fines migration or organic and inorganic precipitation
- Cleaning of gravel packs or screens
- Cleaning of perforations

Finally, Table 2 shows power requirement estimations for cased and open holes, which show that cased-hole wells require six times more power.

Table 2: Power requirement estimations for sufficient US treatment [4, p. 6]

| | ***Cased Hole*** | | ***Open Hole*** | |
|---|---|---|---|---|
| | min | max | min | max |
| *Wellbore diameter [in\|* | 8.5 | 8.5 | 8.5 | 8.5 |
| *Penetration [in]* | 24 | 24 | 24 | 24 |
| *Intensity for cleaning [W/m$^2$]* | 3.7 | 60 | 3.7 | 60 |
| *Intensity at sandface [W/m$^2$]* | 25 | 399 | 25 | 399 |
| *Power transmission fraction* | 0.08 | 0.08 | 0.47 | 0.47 |
| *Intensity in the well [W/m$^2$]* | 307 | 4985 | 52 | 849 |
| *Power in the wellbore [W/ft]* | 32 | 515 | 5 | 88 |

Chapter 2 from “Advances in Ultrasound Technology for Environmental Remediation” by Wu et al. [6] describes the very important cavitation effect that occurs when US in the range of 20 to 100 kHz is applied on liquids.

As discussed before US is a pressure wave that consists of a cyclic series of expansion and compression phases that are generated by mechanical transducers. Compression creates a positive pressure and pushes liquid molecules together. Expansion exerts a negative pressure and pulls molecules apart. Cavitation bubbles (vapor-filled voids) form when pressure amplitude is larger than the tensile strength of the liquid during the expansion phase. Impurities in liquids like particles or dissolved solids, represent weak points where nucleation of these bubbles will occur. When applying a high intensity ultrasonic field, cavitation is transient (unstable) leading to the growth of the bubble until it is unstable and eventually collapses during the compression cycle (Figure 1).

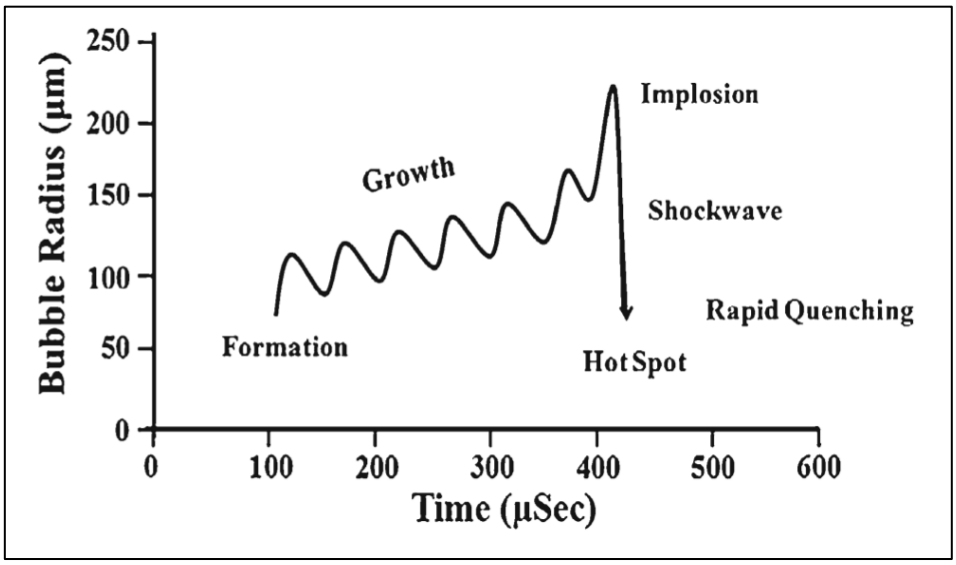


Figure 1: Cavitation bubbles from formation to implosion – bubble radius vs time. [6, p. 7]

Cavitation bubbles concentrate the diffused sound energy and grow rapidly until no more energy can be absorbed which results in an implosion of the cavity. Each implosion then acts as a hotspot and generates energy. Temperatures and pressures in these points can rise up to 5000 K and 500 atm, respectively. Due to these enormous local temperatures and pressures high energy chemical reactions (sonochemical) and physical effects (sonophysical) can occur. Multiple parameters like US frequency and intensity, solvent characteristics, gas properties, external pressure and temperature can affect cavitation. For example, high frequencies will reduce the cavitation effect while increasing the intensity will lead to more violent bubble collapses. Cavities are more likely in solvents with high vapor

pressure, low viscosity and low surface tension. The presence of soluble gas will increase the amount of bubbles but lead to less violent implosions. High external pressure reduces vapor pressure and demand an increase of intensity to create cavitation.

Physically, US produces fluid movements that enhances mass transfer between solid-bulk and gas-bulk interfaces. This movement is created by sonophysical effects that can be explained by microstreaming, microstreamers, microjets and shock waves. They result in turbulences in the fluid stream and a microscale velocity gradient nearby the implosion. Formation of microjets due to the asymmetric collapse of cavities is the most significant effect for US treatment. They produce an asymmetric shockwave with speeds in order of 100 m/s resulting in erosion on surfaces and de-clustering of particles. Sonophysical effects can support various mixing, breaking down of particles and macromolecules, polymer degradation, desorption, extraction, and cleaning processes.

To further understand US signals, John Fuchs [7] from Blackstone-NEY Ultrasonics describes in a comprehensive presentation the technology behind ultrasonic cleaning. He provides an insight into ultrasonic theory and most importantly gives an explanation of ultrasonic cleaning equipment. He further declares how to adjust process parameters and operational procedures to achieve maximum cleaning effectivity.

An ultrasonic cleaning apparatus basically consists of an ultrasonic power supply (generator) that converts standard grid power with frequencies of 50 or 60 Hz to ultrasonic frequencies, and a converter (transducer) that converts this electrical energy to mechanical vibrations. Recent developments in generator technology give a wide variety of possible adjustments of output parameters like square wave outputs, pulsing US energy on and off or frequency sweep. Square wave output for example would increase the number of harmonics in the ultrasonic signal resulting in a multi-frequency system. Introducing high pulsing with shut off intervals of several hundred times per second would increase the amount of high energy bursts and enhance the cleaning process. Frequency sweep is a modulation around a central frequency which especially helps cavitation in terpenes and petroleum based products. A combination of these parameters even can improve cavitation further.

US transducers convert an electrical signal to a mechanical vibration. This can happen magnetostrictive or piezoelectric. Magnetostrictive transducers use a dual energy conversion system: first, from alternating electrical energy to an alternating magnetic field with the help of a coil; this magnetic field then induces vibrations in resonant strips of nickel or other magnetostrictive materials attached to the transducer's surface. On the other hand, piezoelectric transducers use the piezoelectric effect for a direct conversion. Vibrations are created when an electric charge is applied to a piezoelectric material, which then oscillates with the same frequency as the electrical signal. Due to this direct conversion, piezoelectric transducers are more effective and reliable and therefore mainly used in today's applications.

Fuchs concludes his ideas with some process parameters that influence cavitation and therefore the cleaning effectivity. Next to the most basic parameters temperature, time and

chemical composition he also mentions viscosity, solubility of gas, diffusion rate and vapor pressure.

Some interesting experiments and scientific observations were conducted by Gaitan et al. [8] in 1991. His paper “Sonoluminescence and Bubble Dynamics for a Single, Stable, Cavitation Bubble” discusses the phenomenon of sonoluminescence and links it to radial pulsation of bubbles at high pressure amplitudes.

Sonoluminescence (SL) is a weak light pulse during the collapse of cavitation bubbles that can occur due to abnormal high temperatures generated by the fast compression of these bubbles caused by an US field. The study shows a range of SL-active bubble radii above a pressure limit where these light emissions can be observed. This is done experimentally by comparing the phase of SL relative to the sound field to the phase of bubble collapse, which is assumed by theories of radial bubble pulsation.

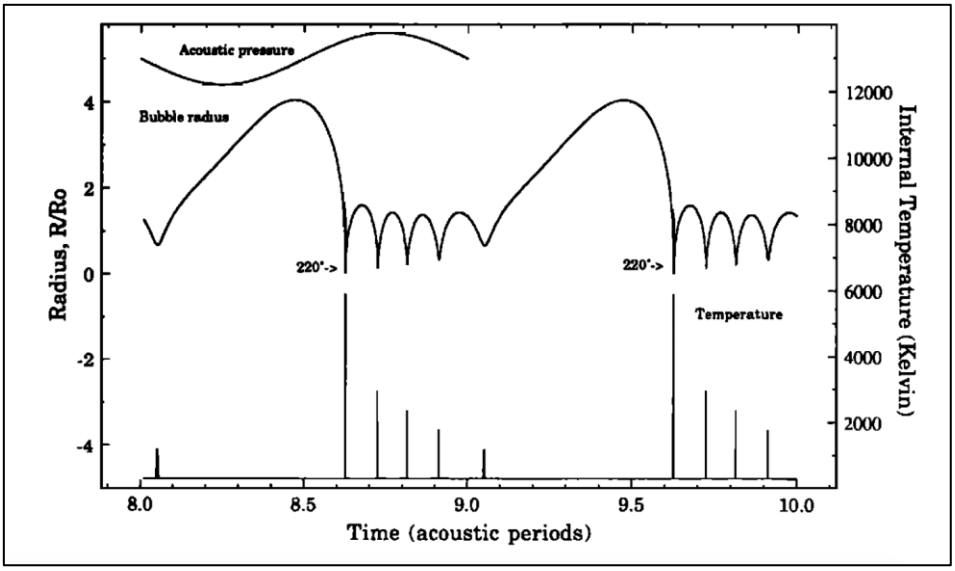


Figure 2: Radius/Temperature vs. Time curves plotted after Prosperetti’s equation showing the characteristic profile of a single bubble in an acoustic field. [8, p. 3169]

three different formulations are compared to describe bubble pulsation: Keller-Miksis [9] radial equation with a linear polytropic exponent; the Keller-Miksis radial equation with the more exact formulation for the internal pressure due to Prosperetti et al. [10]; and Flynn's formulation which includes thermal effects inside the bubble [11]. They all describe the motion of a single bubble in an acoustic field that varies sinusoidally in time. It shows that these pulsations form a characteristic profile which is shown in Figure 2 (center curve). One can determine a relatively slow expansion at the beginning of the US cycle followed by an immediate collapse with several rebounds at the end. In the bottom curve of Figure 2 large temperature spikes can be observed. They correspond in time with the violent, nearly

adiabatic collapses of cavitation bubbles, which also represent the points where SL is generated.

In summary, radial pulsation of bubbles at high pressure amplitudes depend on three quantities: the maximum response or pulsation amplitude ($R_{max}$), the phase of the collapse ($\phi_c$) and the number of minima (M). For a detailed look at the calculations, the interested reader is referred to Ref. [8].

Duhon and Campbell in 1965 were the first to experimentally demonstrate the feasibility of US treatment to influence liquid flow through a porous medium. They executed a series of water flood experiments on an oil saturated sandstone core while applying ultrasound at frequency ranges of 1, 3.1 and 5.5 MHz [12].

Results showed that ultrasonic energy had a major influence on the recovery of oil and the displacement efficiency due to a more uniform displacement front. They yielded additional recovery compared to a waterflood without ultrasound excitation ranging from 6 to 14 percent, reaching a higher recovery with decreasing viscosity and frequency. Further effect was a drop in permeability ratio which suggests a reduction of mobility ratio and an improvement in sweep efficiency. These effects were explained by localized pressure surges during cavitation and oscillating bubbles that force trapped oil into nearby pores.

### 2.1.2 Enhanced Oil Recovery

In 1994 Beresnev and Johnson [13] published a comprehensive review discussing influences of low to high frequency acoustic waves on liquid flow through porous media. They suggest two main applications which are near wellbore cleaning and enhanced oil recovery.

First of all, they discuss principals of fluid movement in the reservoir and how to enhance it. Fundamentally, fluid flow is explained by gravitational and capillary forces. Different densities of saturation fluids in the medium cause gravitational forces that lead to the separation of oil from water. Further, capillary forces are important as they drive liquid percolation through fine pore channels. A flow restriction is created as liquid films adhere to the pore walls and reduce the effective diameter of pore throats which hinders normal percolation or even blocks any flow. The critical attribute in saturated reservoirs are the relative permeabilities between the phases. Research shows that excitation by elastic waves can change these phase permeabilities and enhance mobility of oil below residual oil saturation significantly. The reason for this is that vibrations of the pore surface reduce the adherence of fluids, destroy the surface films and consequently increase pore throat diameters. Further improvement of fluid flow is explained by other appearing effects like in-pore turbulences, acoustic streaming and cavitation. Also, reduction of surface tension and fluid viscosity due to heating of the medium as ultrasonic energy is dissipated helps percolation. In general, these effects can only be observed in medium to high frequency ranges. Especially in procedures for removing wellbore damage due to scales and precipitants only high-intensity, high-frequency US is suitable as it just requires a mechanical destruction of deposits.

Numerous laboratory experiments were conducted by more than hundred researchers: US frequencies ranges between 1 Hz and 5 MHz whereas the main focus lies between 15 and 100 kHz. Sonic field intensities are found between $10^{-3}$ and $10^{4}$ W/m$^2$. Duration of excitation lies between 2 minutes and more than 90 hours. Whereby the duration of effect after US treatment can last from several minutes to a couple of months. As diversified these parameters are as astonishing it is that most of the experiments approved the same outcome: An increase of oil percolation rate through a sample, an increase of oil mobility and relative permeability, a decrease of viscosity, removal of deposits and finally an overall increase of productivity. But not only laboratory experiments showed success but also field tests with acoustic treatment of productive wells proved effective restoring of permeability of reservoirs that were damaged by mud penetration and deposits of scales and salts. Also, the removal of paraffins and asphaltenes was confirmed. Further, ultrasound has successfully been used for preventing salt precipitations on downhole equipment. [14]

In Summary, ultrasonic treatment is reported to be successful in 40 to 50% of the cases studied, and the effects of the improved permeability may last for several months.

Successful field experiments were conducted by Mullakaev et al. over a period from 2010 to 2012 and results were published in the Journal of Petroleum Science and Engineering in 2015 [15]. They provided practical evidence directly from the field that showed the viability of ultrasonic downhole stimulation.

First focus lied on the development of high-efficiency ultrasonic equipment and suitable mathematical modelling of physical processes. To be able to design such vibration system, which in this case is a magnetostrictive transducer, its dimensions should carefully be calculated to meet frequency requirements and guarantee an effective ultrasonic treatment. To achieve maximum values of vibration the frequency of its mechanical resonance should be in the frequency range of the electrical resonance of the generator. Therefore, the natural frequency is calculated by the homogenous Helmholtz equation **eq. 8** [15, p. 202] which is consequently solved with the finite element method.

$$\nabla\left(-\frac{1}{\rho_m}\nabla p\right) - \frac{\omega^2 p}{\rho_m c^2} = 0 \qquad (8)$$

p acoustic pressure [N/m$^2$]; $p = p_0 e^{i\omega t}$
$p_0$ amplitude of acoustic pressure [N/m$^2$]
$\rho_m$ density of the medium [kg/m$^3$]
c sound velocity [Pa]
$\omega$ angular frequency [Hz]; $\omega = 2\pi f$
f natural frequency [Hz]

To verify and further increase the accuracy natural frequencies in the range from 0 – 20 kHz were determined experimentally. Results show that the mode of longitudinal vibrations with three nodes correspond to 19,968 Hz compared to the natural frequency of the entire vibration system of 19,968 Hz. The final design of downhole module consists of two magnetostrictive transducers with a diameter of 42 mm and 102 mm, respectively. They are hollow cylindrically shaped to be able to transform excited longitudinal elastic vibrations into radial vibrations that affect the near-wellbore region, Figure 3 and Figure 4. The ultrasonic generator at the surface consists of a power supply unit; amplifier unit; biasing unit; and control unit. With this design operations in the frequency range from 13 to 26 kHz at a radiated acoustic power from 2 to 10 kW are possible.

Additionally, the authors suggest some criteria for selecting wells that predictively show that ultrasonic treatment of the near wellbore region could work. They are summarized in Table 3. These criteria are fulfilled in Russia for fields in Western Siberia and Samara Region and representing a high viscosity oil field in the United States in Utah, Green River Formation. Well stimulation then was conducted during scheduled repair to reduce total expenditures. The frequency rating was 20 kHz, testing power yielded 10 kW, unfortunately no hints concerning treatment duration are given.

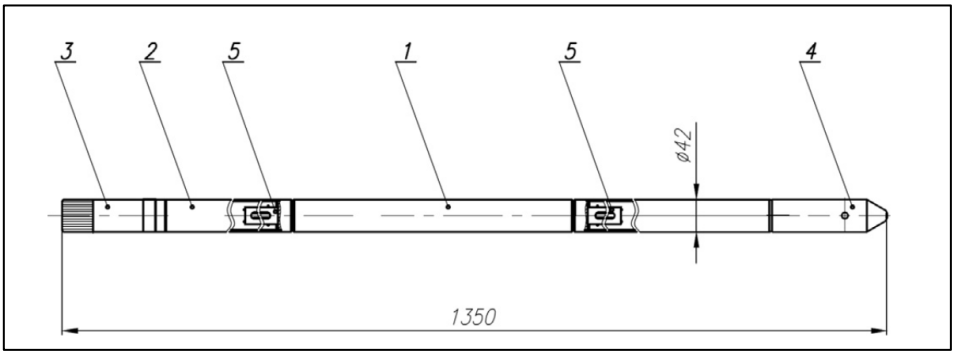


Figure 3: Downhole tool for ultrasonic stimulation: 1 – waveguide; 2 – cable lug; 3 – transport plug; 4 – fairing; 5 – magnetostrictive transducer. Dimensions in [mm]; [15, p. 202]

Table 3: Criteria for selecting wells for US treatment.

| ***Well characteristics*** | ***Value*** |
|---|---|
| *Decrease in formation pressure from initial one, %* | < 25 % |
| *Current water cut, %* | < 80 % |
| *Number of interlayers in the perforated interval* | < 10 |
| *Minimum thickness of producing formation, m* | 3 m |
| *Spontaneous potential* | > 0.5 |
| *Clay content, %* | > 15 % |
| *Decrease in oil production rate for the last 1 – 2 years* | > 2 times or more |
| *Dynamic viscosity under formation conditions, mPas* | < 25 mPas |

Concluding effects for Russian oil fields were a production rate increase of 4.4 and 10.2 tons per day; an increase of well productivity index of 33% and a decrease of water cut by 4%. Overall success rate was 90%. High viscosity oil fields in the United States after stimulation showed a production rate increase of 4.5 tons per day lasting at least for 6 months.

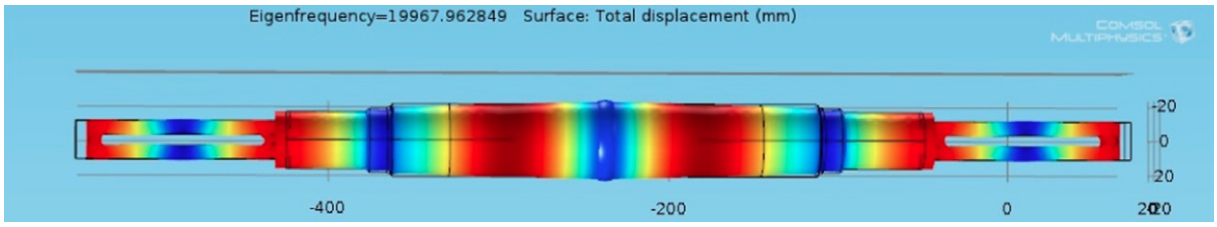


Figure 4: Waveguide radiating system with five nodes. [15, p. 203]

Jeehyeong et al. [16] conducted laboratory tests to investigate the influence of acoustic waves to enhance flow rates through a porous media. They chose a different but very interesting approach to determine the effectiveness of ultrasound treatment by defining nine different influencing factors ($\alpha_i$) and verifying them with the reconstructed permeability equation under different test conditions. A schematic of the test apparatus is shown in Figure 5 and consist of a 500 W ultrasonic processor, a generator to transform conventional grid power to a 20 kHz 1,000 V electrical signal and a vibrator to mechanically operate at 20 kHz. The defining influencing factors ($\alpha_1$ - $\alpha_9$) are shown in Table 4.

For the evaluation of the influencing factors and the effectiveness of the ultrasonic stimulation, the well-known Darcy equation was modified to **eq. 9** [16, p. 148]**.**

$$V = Ki = C\frac{1}{\nu}D_{10}^{2.32}C_u^{0.6}\frac{e^3}{1+e}i \qquad (9)$$

Results show beside that ultrasound significantly enhances flow rate in general that the major influencing factor is definitely the hydraulic gradient. Especially when applying a high-power US signal. Additionally, liquid kinematic viscosity shows a relevant influence in this case. Concerning relatively low US power most governing factor is void ratio, which is most sensitive to soil type and particle distribution.

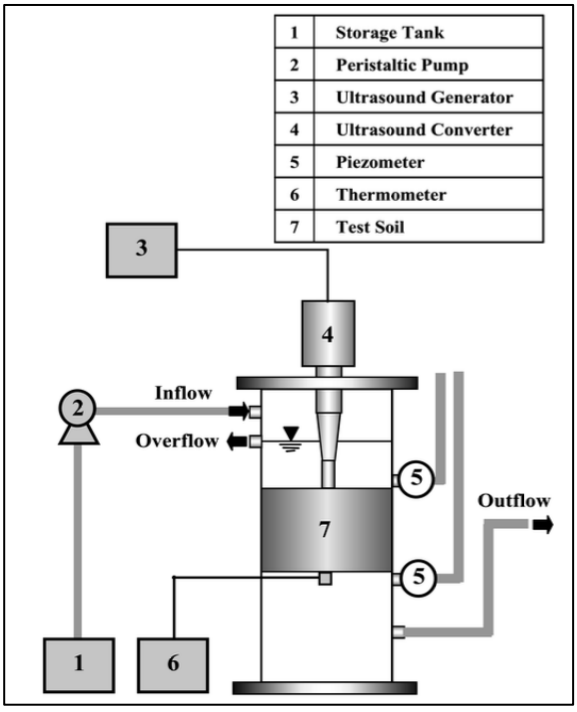


Figure 5: Schematic of test setup.

Table 4: Influencing factors and parameters.

| ***Rate of change*** | ***Influencing factor*** | ***Explanation*** |
|---|---|---|
| $\alpha_1$ | $V$ | Flow rate |
| $\alpha_2$ | $K$ | Permeability coefficient (hydraulic conductivity) |
| $\alpha_3$ | $i$ | Hydraulic gradient |
| $\alpha_4$ | $\nu$ | Liquid kinematic viscosity |
| $\alpha_5$ | $D_{10}$ | Effective grain size |
| $\alpha_6$ | $C_u$ | Uniformity coefficient |
| $\alpha_7$ | $E = \frac{e^3}{1+e}$ | |
| $\alpha_8$ | $e$ | Void ratio |
| $\alpha_9$ | $k$ | Intrinsic permeability |

Noruddin et al. [17] performed a series of laboratory experiments to investigate the influence of intermittent ultrasonic stimulation compared to continuous radiation which commonly is found in EOR. In addition, they used the ultrasonic treatment together with a Surfactant-Polymer Flooding (SPF) process which is a state of the art enhanced oil recovery method.

They found out that the mechanical effect from ultrasonic waves work mutually with the chemical effect from SPF to reduce interfacial tension and enhance oil recovery. Comparing SPF with and without US excitation made clear that residual oil saturation ($S_{or}$) could be further reduced under US stimulation and yielded a 6% lower value. An even lower residual oil saturation could be achieved using intermittent radiation instead of continuous treatment. $S_{or}$ reached 39.6% compared to 41.7%. Further, energy consumption was reduced during intermittent stimulation and therefore an increase in cost efficiency could be achieved.

In a series of papers [18] [19] [20] [21] Hamida and Babadagli investigated the influence of high-frequency, high-intensity ultrasonic waves on capillary imbibition. They conducted numerous laboratory experiments using Berea Sandstone and Indiana Limestone plugs which are 2.5 cm in diameter and have a length of 5 cm. Two different coating setups were used: to obtain a counter-current imbibition all sides except one is coated with epoxy; for a co-current imbibition, all sides are left open to flow. Cores are saturated with different oleic phases and put in an ultrasonic bath with different aqueous phases. Observed fluid pairs are: air-water, mineral oil-brine, mineral oil-surfactant solution and mineral oil-polymer solution. Final monitored value is the recovery rate due to capillary imbibition. Driving forces in such experiments are expected to be interfacial forces only, such as IFT, wettability and pore radius.

In the first series of tests [18] US frequency was 40 kHz at an approximate operation power of 2 kW. Hamida and Babadagli expected an enhancement of fluid flow when US is applied due to the change of wettability, reduction of viscosity, reduction of IFT, increase of permeability and peristaltic transport due to deformation of pores, removal of fine particles,

coalescence of oil drops due to Bjerknes forces and excitation of trapped oil drops due to cavitation. To verify these assumptions, they used a generalized form of the exponential transfer function from Cil et al. **eq. 10** [22, p. 6]:

$$\frac{R}{R_\infty} = 1 - e^{-\omega t^n} \qquad (10)$$

$R$ Recovery [%]
$R_\infty$ Ultimate recovery [%]
$\omega$ Convergence constant [$t^{-1}$]
$n$ Exponent
t Time [t]

where $\omega$ and $n$ are the parameters in main focus, as they are functions of rock and fluid properties and control the capillary imbibition rate. Analysis showed that US affects $\omega$ much more than $n$ as $n$ is just a tuning parameter of recovery rate which is mainly controlled by wettability and permeability. On the other hand, $\omega$ is highly affected as it links to IFT and core dimensions. Especially when considering high IFT fluid pairs, strong alterations of $\omega$ were observed which verifies that US mostly affects IFT between aqueous and non-wetting phase when viscosity is held constant. That in the end leads to a higher oil recovery.

In Summary, almost all experiments showed an enhancement of final capillary imbibition recovery under ultrasonic waves. Only air - water fluid pairs were an exception. Wettability seemed not to be affected by US. IFT showed the highest change during ultrasonic radiation and therefore has the strongest influence on recovery rate.

In their second approach [19], the chosen fluid pairs were mineral oil and different anionic and nonionic surfactant solutions above and below the critical micelle concentration (CMC). Representing a viscoelastic solution, they also used Xanthan gum as aqueous phase. Further investigations are made with the alteration of ultrasonic intensity, representing a LO and a HI case with 25 W/cm$^2$ and 45 W/cm$^2$ respectively. Ultrasonic frequency was set to 20 kHz.

First results showed an increase in system temperature with higher intensities and longer exposure time (Figure 6). A consequent effect is the increase of ultimate recovery as fluid viscosity and IFT is reduced as shown in Figure 7. Limitations are found with higher polymer concentrations (Xanthan Gum) as a lower recovery with increasing intensity is observed, proving that US has a substantial effect on polymer rheology which stipulates an optimal ultrasonic intensity.

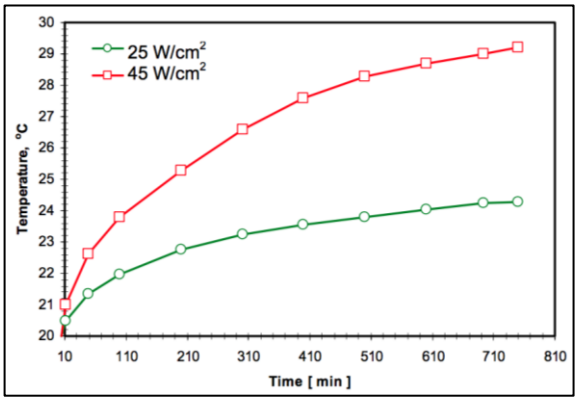


Figure 6: Change of system temperature over time under LO and HI ultrasonic intensity. [19, p. 7]

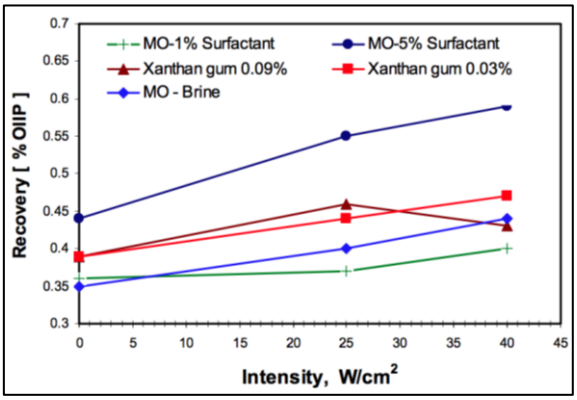


Figure 7: Alteration of ultimate recovery with increasing ultrasonic intensity. [19, p. 9]

Further clarification is obtained when comparing recovery rate and ultimate recovery from the control experiment (no US stimulation) with different intensity cases. The non-ultrasonic experiment recovered 35% OOIP at a rate of 0.06% per minute. LO case showed an insignificant change in recovery rate but an UR increase of 5% while the HI case yielded an increase of final recovery of about 9% with a slightly larger increase of the rate. Reasons for that increase are vibrations in the rock matrix that disperse fingering and percolation and thereby creating a more uniform displacement front. Variations of ultimate recovery are also found with different anionic surfactant concentrations. A 1% surfactant for example showed no significant increase of recovery, whereas a surfactant above CMC with 5% showed an increase of up to 11%. Possible explanations are the effect of US on the surfactant absorption onto the rock matrix which is reduced and therefore weakens the surface film in the pore throats. Further, US accelerates micro-emulsion generation above CMC and also increases the solubility into oil which strongly decreases IFT.

In conclusion, in all cases except for Xanthan gum US enhances recovery of oil directly proportional to the applied intensity.

In another set of experiments, Hamida and Babadagli [20] [21] performed beside their well-known capillary imbibition tests a series of viscous displacement (Hele-Shaw) experiments. They wanted to show the impact of high-frequency, high-intensity ultrasonic radiation on the immiscible and miscible displacement in porous media by eliminating the effect of interfacial forces and maximizing the viscous forces. To reach that effect, low IFT solutions or miscible fluids are injected in a Hele-Shaw cell to displace the oil. To analyze the results fractal techniques including fractals and lacunarity are used.

In general displacement of fluids with different viscosities, patterns known as “viscous fingers” occur. Figure 8 shows such frontal patterns achieved by the Hele-Shaw experiment for water (a,b) and anionic surfactant (c) injected into mineral oil at different rates with and

without ultrasonic radiation. As seen in Figure 8 (a) more fine fingers and a higher sweep efficiency close to the injector is achieved under US. At lower injection rates (b), molecular diffusion is enhanced under US which is shown due to wider, shorter fingers that tend to branch out from larger fingers. Surfactant injection showed the opposite behavior (c). That leads to the result that US stabilizes the liquid-liquid front of high interfacial tension fluids, but generates larger instabilities when interfacial tension is low. Therefore, IFT is the most sensitive parameter to ultrasonic radiation in viscous displacement.

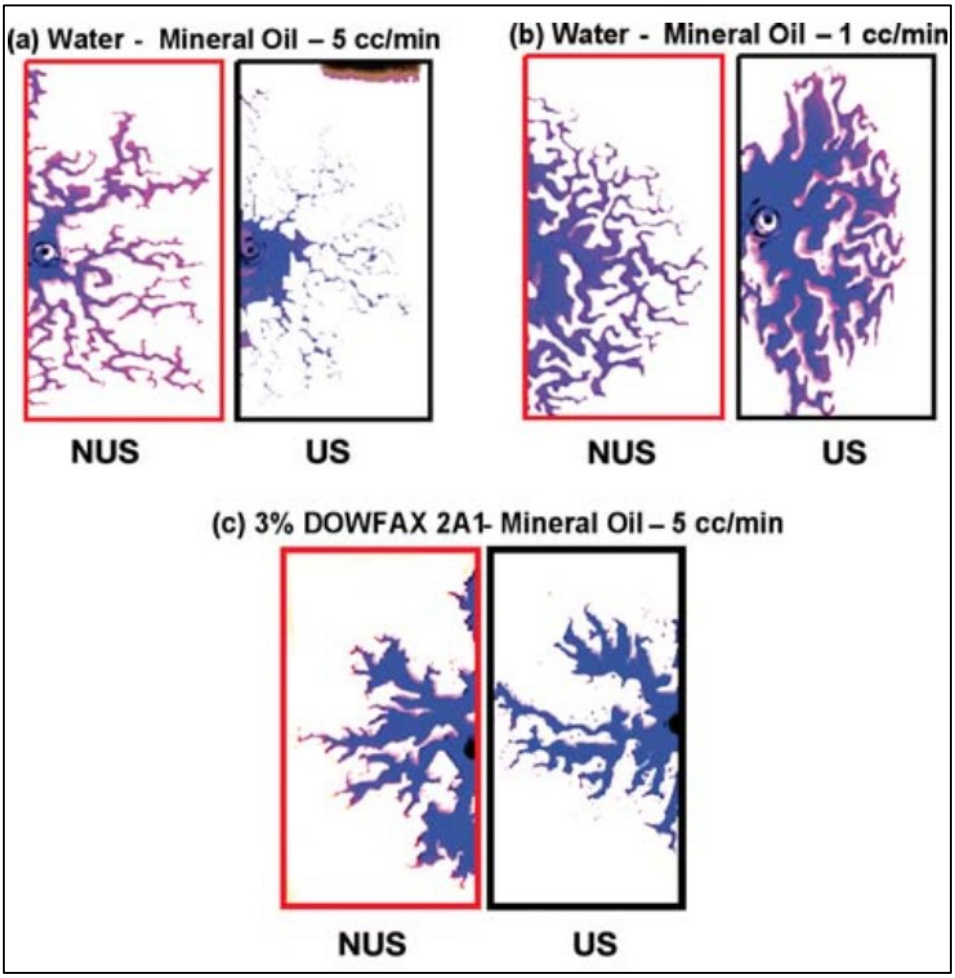


Figure 8: Comparison of Hele-Shaw patterns under ultrasound (US) and non-ultrasound (NUS) radiation. [21, p. 18]

In 2002, Poesio et. al. [23] also investigated the influence of high frequency acoustic waves on laminar flow in porous media. They especially wanted to determine the main effect responsible for the decreasing pressure gradient during wave propagation.

Therefore, they conducted experiments in which 100 to 300 mD Berea sandstone plugs were pressurized in a steel vessel to reach downhole conditions. At about 150 bars the pressure is

high enough to avoid cavitation. Then a constant flow of brine was pumped through the plug. An ultrasonic signal with a frequency of 20 and 40 kHz and a power of 2 and 0.7 kW was applied. Consequently, three pressure drops, temperature in the middle and the front of the core, the constant flow rate, and amplitude and frequency after the core was recorded.

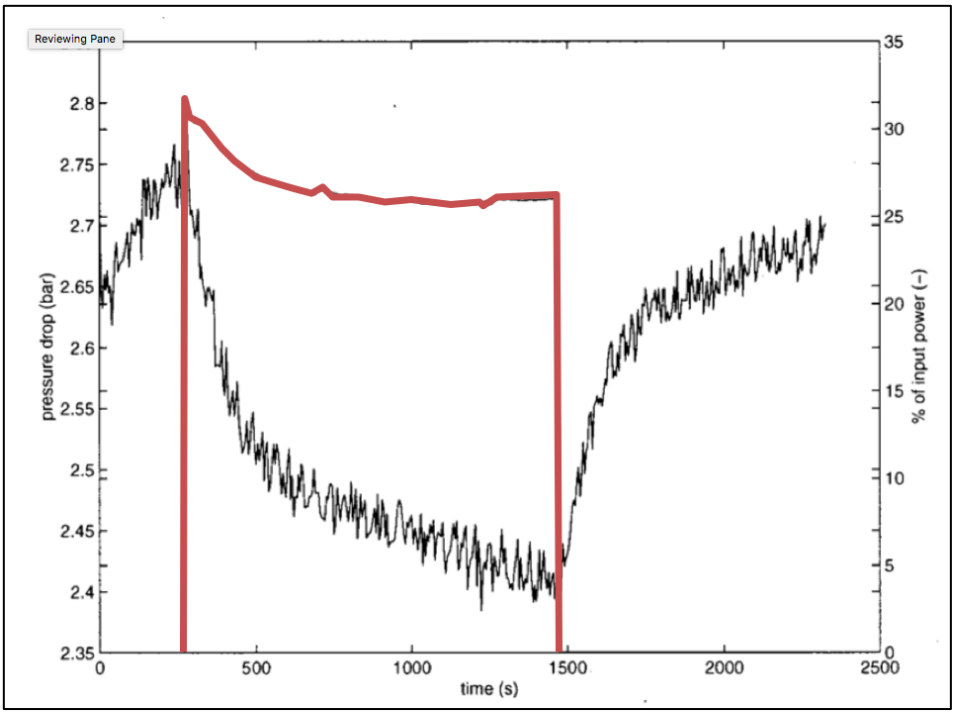


Figure 9: Black line: pressure drop of the middle part of the core; red line: percentage of power output. modified [23, p. 2021]

As expected Figure 9 shows the actual pressure drop over the middle of the core and the applied acoustic power both as a function of application time. To explain that gradient, calculation with the well-known Darcy equation were made to determine effective permeability. Without taking the observed temperature increase in concern it seemed that effective permeability significantly increased under ultrasonic radiation. However, by including this temperature effect in the calculations it showed that permeability remains basically constant. In fact, the only effect that explains the pressure drop is the decrease of liquid viscosity caused by the increase of temperature as acoustic energy gets dissipated.

To further verify this observation theoretical calculations were conducted. First, temperature as a function of time is predicted by solving the heat balance equation **eq. 11** [23, p. 2023] assuming thermal equilibrium and temperature being a function of axial coordinate only due to sufficient radial insulation. Results showed that calculation compared well with the experimental observations.

$$\left[\rho_f c_{p,f}\phi + (1-\phi)\rho_s c_{p,s}\right]\frac{\partial T}{\partial t} + \rho_f c_{p,f} v \frac{\partial T}{\partial x} = \kappa \frac{\partial^2 T}{\partial x^2} + S_{heat} \qquad (11)$$

$T$ Temperature
$c_{p,f}$ Specific heat of fluid
$c_{p,s}$ Specific heat of solid
$\rho_f$ Density of fluid
$\rho_s$ Density of solid
$v$ Superficial velocity of the liquid
$\phi$ Porosity
$\kappa$ Effective diffusion coefficient
$S_{heat}$ Source term

In the last step, assuming constant permeability and the temperature dependence of viscosity, pressure drop can be calculated with Darcy equation **eq. 12** [23, p. 2023]

$$\frac{dp}{dx} = -\frac{\mu}{K} v \qquad (12)$$

$\frac{dp}{dx}$ Pressure drop
$\mu$ Superficial liquid viscosity
$K$ Permeability
$v$ Liquid velocity

Likewise, results showed good accordance with experimental observations concluding that the decrease in pressure gradient can be explained completely by the decrease of fluid viscosity caused by a temperature increase when ultrasonic energy gets dissipated from the rock.

A study with a lot more theoretical background was conducted by Aarts and Ooms [24]. They worked on a numerical model to describe the mechanism of the deformation of pore walls in the shape of travelling transversal waves when US is applied. This deformation induces a net flow of fluids inside the pores caused by peristaltic transport. This enhancement of liquid flow by ultrasonic radiation was then verified experimentally. To finally be able to judge the feasibility of ultrasonic radiation they compared the flow rate of peristaltic transport to the rate of a Poiseuille flow due to a pressure gradient.

In the theoretical model wave speed c and wave amplitude a are strongly linked to the power output P of the acoustic generator and the shear modulus G of the porous media. The compressibility $\kappa$ of the liquid acts as a dampener on the net flow. A perturbation analysis was performed to solve a system of Navier-Stokes equations to predict the flow. For detailed insights to the governing equations refer to reference [24, pp. 2-4].

A comparison of induced flow due to US leading to peristaltic transport with a Poiseuille flow caused by a pressure gradient of $10^6$ Pa/m showed very similar results which indicates that induced flow is not solely a result of peristaltic transport. Other reasons for the flow enhancement were suggested to be non-linear effects like acoustic cavitation or acoustic streaming. However, no more insights were given into these assumptions.

Experimental results proved that flow velocity has a strong almost linear relation to the power output of the generator which agrees with numerical predictions. Thus, the dependency of flow on hardness of the medium (shear modulus) could not be validated and therefore peristaltic transport became doubtful.

China's heavy oil fields are one of the few areas in the world in which on-field pilot tests for ultrasonic stimulation were conducted. Especially Xiao et al. [25] in 2004 summarized results from previous stimulations. Further, they effectively performed numerous field test themselves that proved the high potential of acoustic radiation to enhance oil production and/or ultimate recovery. They used a quite simple system consisting of an ultrasonic power generator, a cable applicable for downhole conditions and a piezoelectric transducer which is lowered to the pay zone of interest. Unfortunately, no detailed information about treatment duration, treatment ultrasonic frequency or power intensity are provided.

Results for 10 ultrasonically treated producers in the Shengli oil field showed an increase of daily liquid production rate of about 40% which is explained due to a reduction of oil viscosity and an increased flow velocity. In the Daqing oil field ultrasound treatment started in 1989 where 9 of 13 producers showed a significant enhancement of liquid production rate from 46 tons per day to 137 tons per day in total. The Zhongyuan oil field, where most reservoirs are very complex, having a low permeability, and showing a strong heterogeneity, many conventional stimulation methods showed to be ineffective. US stimulation in contrast showed an average 4.7% increase of daily oil production of 12 treated wells. In the Huabei oil field main improvements of oil production by US stimulation were reached because of oil demulsification. 170 wells were successfully stimulated in the Yumen oil field over a period of six years making ultrasonic vibration treatment the most used and most effective production technology in this area.

Xiao et al. concluded their research with a basic computer model using a modified heavy oil reservoir simulator. They want to predict the effects of high frequency ultrasonic stimulation on production rate and heavy oil recovery. With the usage of control parameters obtained from the laboratory a better understanding of the change of physical characteristics of the produced fluid and percolation in heavy oil reservoirs is granted. Test simulations showed

promising results that resemble observed results from field tests and other laboratory experiments.

Amro et al. [1] performed a series of laboratory test on core samples to study the effectivity of US to enhance oil mobility. Main focus of this research was to find and understand alternative tertiary recovery methods with lower application risk. Horizontal and vertical core flooding tests at original oil in place (OOIP) and residual oil saturation after water flooding were conducted. Observations made were an increase of oil displacement rate, an influence on relative permeability and water breakthrough and with stimulation at residual oil saturation a higher ultimate oil recovery. Treatment parameters were clearly defined and set to an ultrasonic frequency of 50 kHz with a power output of 300 watts. Treatment time did not exceed 45 minutes and both intermittent and continuous wave stimulation was used. Experiments were conducted using Berea sandstone plugs saturated with Arabian light crude oil. The displacement agent was a synthetic brine with a 5% salt concentration.

Results showed an overall increase in oil recovery. Ultrasonic excitation changes the relative permeability of the rock and enhances the rate of oil production. In horizontal corefloods an early water breakthrough is observed which can be explained by gravitational separation. To avoid this effect stimulation of horizontal wells in the upper part of the reservoir are preferred. At residual oil saturation recovery rate is increased which suggests an US treatment in reservoirs with high water saturation or in depleted reservoirs. Further ultrasonic radiation is not recommended in unconsolidated reservoirs as sand production can occur. Finally, no negative impacts on rock or fluid properties are noticed during ultrasonic excitation.

The concluding potential of US treatment and its superiority to conventional EOR methods are summarized as following: It can replace chemical stimulation which has a high environmental impact and in many cases is not compatible with rock or fluid. It is flexible and can be used at any interval of interest. It is additionally able to remove filter cake or other near wellbore damages. And last but not least it can be performed while the well is producing, therefore, no shut-in time is required.

Another series of displacement experiments as well as one-phase flow experiments were conducted by Mohammadian [26] in 2011. The aim was to clarify the temperature effect during ultrasonic stimulation and to find the main reasons for a recovery increase.

During sonication, severe temperature rises were observed. At a treatment time of about 140 min temperatures rose between 4°C, 12°C and 16°C to the respective ultrasonic power output of 100 W, 250 W and 400 W. Fluid properties that are affected by temperature are viscosity and interfacial tension. Although the decrease of IFT was notable, the reduction was too small to affect the capillary number and therefore does not contribute to the reduction of residual oil nor increase the recovery. Hence, the reduction of viscosity should be one of the main influencing factors contributing to the flow enhancement. This also is verified by the one-phase flow experiment where a reduction of pressure gradient is

observed which is explained due to the reduction of fluid viscosity seen in **eq. 13** [26, p. 4]. As the parameters Q, L, K, A and φ are constant only the viscosity μ can be affected.

$$\Delta p = \frac{Q\mu L\varphi}{KA} \qquad (13)$$

$\Delta P$ Pressure drop
$L$ Length
$A$ Cross-sectional flow area
$\mu$ Liquid viscosity
$K$ Permeability
$Q$ Flow rate

Further observations were the formation of emulsions. During ultrasonic stimulation, they were unstable thus the phases were completely separated after 3 hours. This leads to the conclusion that the reduction of viscosity and the emulsification are main factors enhancing oil recovery under acoustic treatment.

### 2.1.3 Cleaning

The following section deals with the removal of contaminating material from the wellbore and near-wellbore region and discuses ultrasound cleaning in general.

Near-wellbore formation damage can occur during the entire lifecycles of a well, including drilling, completion and production. It has a major effect on the productivity of a well as it dramatically reduces effective permeability and can lead to total plugging and to obstruct production permanently. Near-wellbore damage is associated with any kind of transport of colloidal solids into or out of the wellbore and is different from well to well. Usual preventative actions for such damage caused by drilling, completion or injection is an expensive pre-treatment of the fluid. Whereas, this will not hinder any damage arising from the plugging of pores resulting from fines migration during production. Different treatment methods are acidizing or fracturing. These measures are expansive and have a major environmental impact. Also, precipitation from paraffins, asphaltenes, waxes and different types of scaling can drastically affect production and count as wellbore damage. Mechanical, thermal or chemical cleaning treatments are available to remove such contaminations, but they also include environmental concerns and lead to high costs. Although these conventional well stimulation techniques have been applied successfully, they all have significant limitations. Therefore, ultrasonic treatment to reduce wellbore damage is intensively investigated and may be implemented in the field as wireline deployable tool.

Venkitaraman, Roberts and Sharma [27] conducted a feasibility study of using ultrasonic radiation to reduce formation damage of the near wellbore zone. The investigated damage is caused by fines migration and mud solids plugging the pore throats leading to a reduction in permeability. Laboratory experiments were performed to validate the cleaning effect of ultrasound and determine the dominant mechanism behind it. Acoustic cavitation and acoustic streaming were included in their considerations.

During the experiments brine-saturated cores were damaged with drilling muds or treated with fresh water injection to simulate fines migration. Ultrasonic energy with different frequencies and intensities was then applied. Monitoring of the permeability for three different sections of the core as a function of ultrasonic treatment time started during backflow. Observations concerning increase in permeability, treatment depth and ultrasonic energy requirements were made. The experimental apparatus is shown in Figure 10.

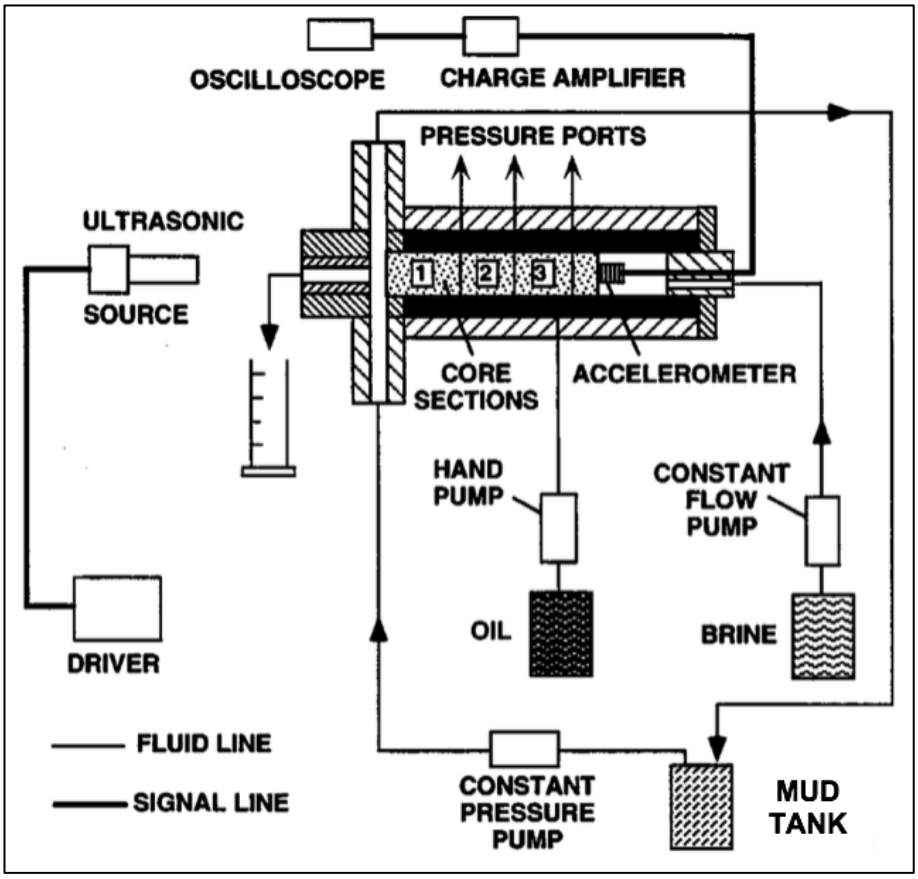


Figure 10: Apparatus and configuration used for damage experiments. Modified [28, p. 20]

The first set of experiments dealing with mud-damage removal showed an influence of US on the first section of the core only which is about 2.5 inches away from the inlet. Further sections are not affected at all. An increase in permeability by factors between 2 and 10 was observed. Both sandstone and limestone as well as water phase and oil phase proved to be positively affected by ultrasonic treatment. In general, permeability increased with increasing ultrasonic intensity, increasing flow rate as well as increasing treatment duration.

The second part deals with fines-damage removal. This type of damage is uniform along the core and affects the permeability measurements of all three sections as opposed to mud-damage which only affected the first one. Results from sonication showed an increase of permeability by a factor of seven although only the first section showed to be affected. This leads to the assumption that treatment depth cannot exceed 2.5 inches and is strongly linked to power output and on the coupling efficiency between source and sample. Further tests showed that an additional permeability increase can be achieved with subsequent treatment under static conditions.

Conclusions of this study, concerning the relative low acoustic intensity, were that acoustic streaming is the dominant mechanism for reducing both types of damages within the pores. Thus, cavitation contributes to the removal of near-surface particles.

In a follow-up paper Roberts et al. [28] presented experimental investigations on applying previously developed [27] ultrasonic techniques on formation damage caused by paraffin precipitation and polymer infiltration.

In this study, mechanical agitation caused by cavitation and/or microstreaming is the main mechanism to remove paraffin deposits. Due to this agitation paraffin crystals get re-suspended and easily can be produced with the oil. Results showed that no improvement of permeability of any section of the core was achieved during low intensity (100 W/m$^2$) treatment. First changes were noticed after six circulated pore volumes with an intensity of about 300 W/m$^2$ and a frequency of 30 kHz; permeability of the first section could be restored to its pre-damaged state. Further improvements were visible after additional sonication with an input acoustic intensity of 1800 W/m$^2$ at 20 kHz: In Section 1, permeability was enhanced immediately from kd/ki factor of 0.4 to 1.2, where ki represents the initial permeability and kd the damaged permeability at different cleaning stages. Section 2 changed from 0.4 to 0.85 after 12 circulated pore volumes. In section 3 no improvement was possible. Total treatment duration was 24 minutes at a cumulative energy input of 1.3 kJ. No significant temperature changes were observed throughout the experiment confirming that cleaning due to temperature effects can be precluded. Improvements are solely achieved due to mechanical excitation leading to resuspension or dispersion, which are effects caused by microstreaming. Cavitation is assumed to help the cleaning process only up to 2 cm into the core as energy dissipation due to attenuation is to large and intensities get too low. Acoustic cleaning of polymer infiltration proved to be much harder and less effective. With 5700 W/m$^2$ a much higher input intensity is required to show improves of sections 1 and 2, yielding a 50 to 70% increase of damaged permeability, whereas pre-damage initial values could not be reached. Therefore, it is recommended to use US together with chemical treatments for a satisfying polymer infiltration removal.

Table 5: Summary of ultrasonic cleaning results and parameters. [28, p. 23]

| | Core Section 1 (6.35 cm) | | Core Section 2 (5.08 cm) | | | | |
|---|---|---|---|---|---|---|---|
| Type of Damage | $k_d/k_i$ Before Sonication | $k_d/k_i$ After Sonication | $k_d/k_i$ Before Sonication | $k_d/k_i$ After Sonication | Input rms Intensity (W/m$^2$) | Input rms Power (W) | Total Input Energy (kJ) |
| Mud | 0.07 | 0.32 | 1.0 | 1.0 | 1500 to 4500 | 0.76 to 2.28 | 1.3 |
| Fines | 0.03 | 0.18 | 0.03 | 0.03 | 1200 to 3000 | 0.61 to 1.51 | 0.7 to 1.4 |
| Paraffin | 0.40 | 1.20 | 0.40 | 0.85 | 300 to 1800 | 0.15 to 0.91 | 0.9 to 1.4 |
| Polymer | 0.22 | 0.37 | 0.53 | 0.78 | 5700 | 2.89 | 12.0 to 14.0 |

To conclude the research Table 5 summarizes the most important parameters from all four types of wellbore damage. The observed acoustic power requirements for effective cleaning provide working specifications for possible ultrasonic devices used in downhole applications.

Insights into ultrasonic surface cleaning are provided by Awad [29]. Main cleaning mechanism is the generation and evenly distribution of cavitation implosions in a liquid medium. High energies get released from these implosions which collide with surface contaminants and decompose the particles. Sequently, dynamic pressure waves carry dispatched fragments away from the surface. This combination guarantees a deep penetration into crevices, blind holes and other spots that are inaccessible for conventional cleaning methods.

Factors of interest that influence the effectivity of ultrasonic cleaning are signal input properties, fluid properties and system properties. They include wave form, frequency and power intensity; viscosity, IFT, density and vapor pressure; medium temperature, pressure and liquid flow regime, respectively. For water at normal conditions a minimum intensity of 0.3 W/cm$^2$ is necessary for a 20kHz signal to be able to produce cavitation. Low frequencies in the range of 20-30 kHz create above this intensity threshold a relative small amount of cavitation, thus providing more energy, which is appropriate to remove heavy and large-size contaminants. In contrast, high frequencies (60-100kHz) produce dense cavitation with low energies suitable for cleaning delicate parts and preventing surface damage.

A comprehensive study of ultrasonic irradiation for treatment of asphaltene deposition and the effect on crude oil viscosity was conducted by Shedid in 2003 [30]. To validate the feasibility for this application two different sets of laboratory experiments were performed: the crude oil experiment (1) with and without solvent effect and the dynamic flow experiment (2) under different treatment durations and frequencies.

In general, asphaltenes are defined as the part of crude oil, which dissolves in toluene. They are polar aromatic compounds, containing fused benzene, naphthalene and phenanthrene rings with a high molecular weight. Asphaltene precipitation can damage rock permeability of sandstones and carbonates and effect capillary pressure and pore size distribution. Ultrasonic treatment causes dispersion of the asphaltene-resin fraction and decreases the size of asphaltene clusters due to thermodynamic changes, which leads to improved production abilities.

In the first experimental setup (1) 18 identical crude oil samples with an asphaltene content of 2.47 wt.%, were sonicated with a constant frequency of 20 kHz. Treatment duration varied between 0 and 30 minutes; system temperature was set to 25, 40 and 60°C. Unfortunately, no information about power intensity is provided. Measurements of oil viscosity and analysis of microscopic images of centrifuged oil samples with asphaltene clusters were performed.

Results are shown in Figure 11. For all time intervals, an increase of temperature leads to a decrease of oil viscosity; for all temperatures, a decrease of oil viscosity is seen in the first 10 minutes of irradiation; between 15 and 25 minutes oil viscosity increases again and at 30 min reaches an abnormal high value.

The first decrease is explained due to the degradation of resin intra-molecular bonds and followed by its separation from asphaltene particles. The viscosity increase after 15 min is

caused by a breakdown of asphaltene clusters into dispersed particles, which increases its solubility in crude oil. After 30 min, the boiling effect contributes to the high viscosity as light components evaporate increasing the asphaltene concentration. Further, the image analysis showed a gradual decrease in asphaltene cluster size with increasing treatment time.

The main conclusion for this experiment is, that treatment time should be selected lasting longer than 10 minutes but stop before the boiling effect occurs.

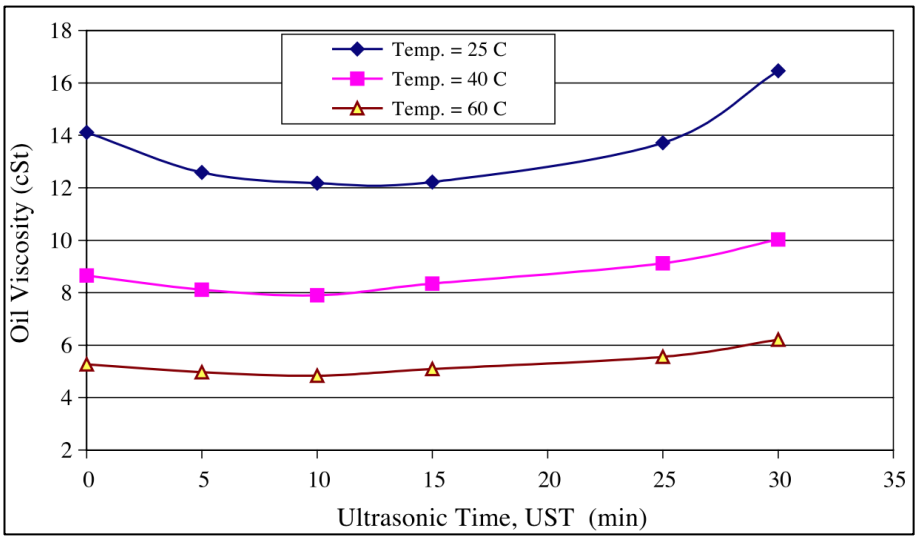


Figure 11: Effect on crude oil viscosity under ultrasonic irradiation with different temperatures and treatment durations. [30, p. 60]

A very similar experiment with 12 samples with different toluene concentrations of 5, 10, and 15 vol.% was conducted. Observations at four different ultrasonic treatment durations at two different temperatures were chosen. Results show a decrease of oil viscosity with increasing solvent concentration at all time intervals and temperatures, which is explained by the increase of asphaltene solubility.

The second experimental setup (2), a dynamic flow experiment, included seven carbonate core samples with damaged permeability due to asphaltene precipitations. Variations in treatment time intervals and ultrasonic frequencies are made. Oil permeability is measured and scanning electron microscope (SEM) images are analyzed.

Results at different time intervals but at a constant frequency of 20 kHz showed an enhancement of oil permeability (Kust) with increasing treatment time, thus the original undamaged permeability (Ko) could not be reached (Figure 12). The analysis of the SEM images indicated an increased surface roughness and appearance of micro cavities which lead to the conclusion that ultrasonic irradiation not only removes deposited asphaltenes but also affects the rock itself to increase its permeability.

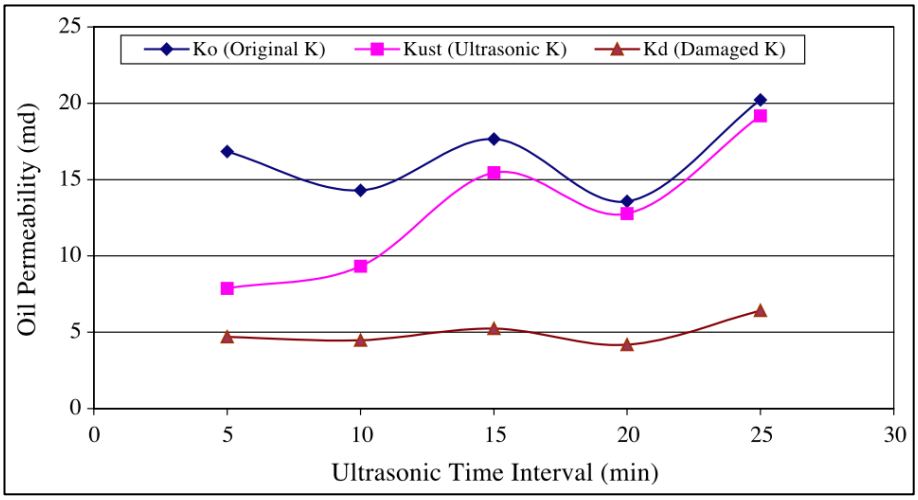


Figure 12: Change of oil permeability under ultrasonic irradiation with different time intervals. [30, p. 65]

When applying different frequencies, one can determine an improvement of permeability with increasing frequencies which end up in an enhanced recovery factor as seen in Figure 13. With increasing frequency, SEM images show more sever surface roughness, deeper micro cavities and a creation of micro fractures.

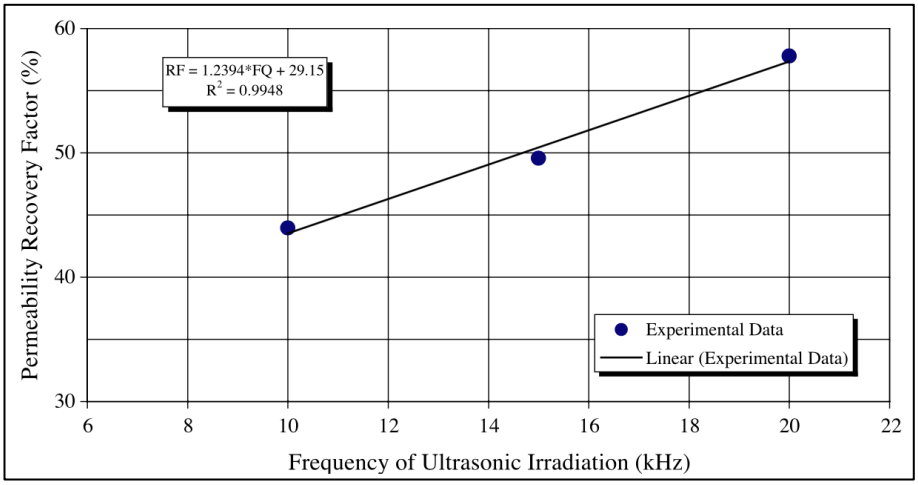


Figure 13: Increase of recovery factor with increasing ultrasonic frequency. [30, p. 68]

Summarizing this study, the proposed ultrasonic technique to treat damaged reservoir permeability shows viability as asphaltene clusters are decomposed to finer particles, oil viscosity is reduced and induced micro-cavities and fractures increase rock permeability

Hofstätter and Pavlov [31] discussed the possibility to use ultrasound for the destruction of resin-paraffin deposits in pipelines. As main cleaning factor, they assumed cavitation as its high energies with large pressures, temperatures and velocities are suitable to destruct contaminants and remove them from hard surfaces.

They conducted a laboratory experiment in which a paraffin contaminated plate is sonicated with an acoustic signal with a frequency of 75 kHz and an amplitude of 10V. Treatment duration was 30 seconds at 6 cycles. Changes were observed with a high-speed camera, shooting with 700 thousand frames per second.

Results showed the feasibility of ultrasonic waves to remove paraffin deposits from steel surfaces. Cavitation and its effect could clearly be detected from high-speed images. Suggestions for application in pipelines are the use of ring resonators, mounted directly on the pipeline. Several ultrasonic stations need to be installed along the pipeline to guarantee effective cleaning.

A very different approach to generate high-power sound waves for damage removal and cleaning purposes was taken by Champion et al. [32]. They used high-voltage electrical discharge in a liquid medium to initiate sound waves. Electrical properties for that high energy pulse reaches energies up to 300 J/Pulse with a maximum operating voltage of 30 kV. The electrical discharge creates a spark which vaporizes the surrounding medium and creates a plasma gas bubble. After discharge, the bubble collapses rapidly and produces shockwaves that propagate and clean the wellbore. Dominant physical cleaning mechanism results from vibrational energy acting on mechanical bonds to remove the plugging material.

Two types of damage are discussed and cleaning effectivity is evaluated with laboratory experiments. First application was the removal of mud cake damage from a Berea sandstone sample. Secondly, they tried to remove plugging material from the surface of a sand screen. For screen cleaning purposes, they used a 360° radial acoustic field which also is perfectly suited for applications inside a wellbore. Therefore, test at ambient conditions but also more importantly at an elevated temperature of 100°C and pressure of 100 bar were performed. For removal of mud cake damage they used a focused acoustic beam at ambient conditions. For focusing reasons different adapters were tested represented by an elliptical shape, a parabolic shape and a conical shape as seen in Figure 14.

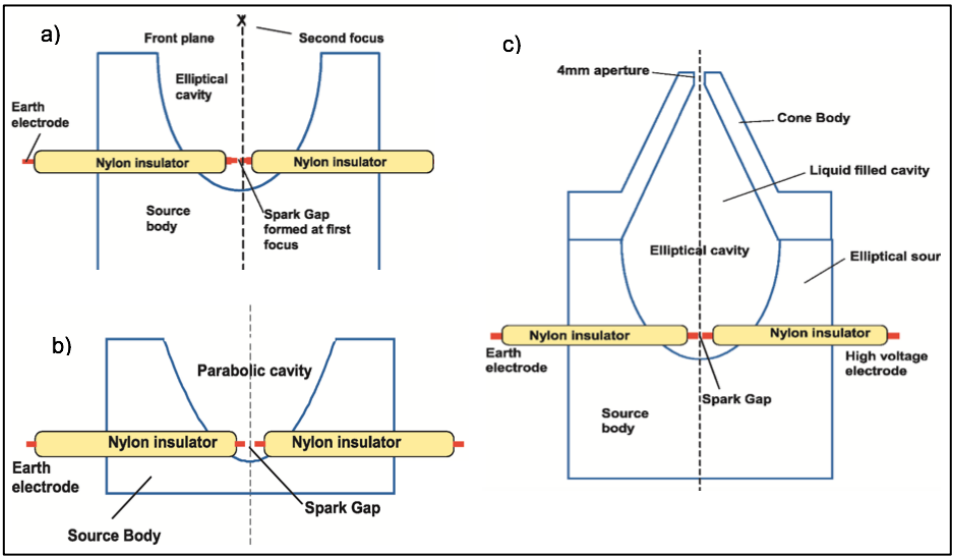


Figure 14: a) Elliptical-cavity acoustic source; b) Parabolic-cavity acoustic source; c) Elliptical-cavity with conical extension. Modified [32, p. 116]

Results of the mud cake removal experiment showed an overall permeability increase and a minimum permeability regain compared to undamaged values of 60%. The CT (Computerized Tomography) density, which indicates rock porosity, reaches an average regain of 80% in some cases even yielding a higher value than virgin CT density. For all tests mud cake removal appeared in a similar way: the mud cake peeled off the core surface either in smaller pieces or large flakes. About 30 different trials for screen cleaning were conducted using varying coating materials, test fluids, pressure and temperature regimes as well as different acoustic pulse intervals and energies. Cleaning efficiency was between 0 and 100% but showed in most cases positive effects. Attenuation of cleaning effectivity was observed with increasing surrounding pressure. Different temperatures showed no effect. An average cleaning factor for ambient conditions was evaluated and yields 10 pulses/cm compared to 100 bar the cleaning factor reaches 30 pulses/cm. For detailed overview of result refer to reference [32].

The main focus of the work done by Wong et al. [33] is to experimentally find the needed acoustic power input to effectively remove formation damage caused by fines and particle plugging under realistic downhole conditions. Subsequently, they designed an adequate downhole acoustic tool for field deployment. Under atmospheric conditions the dominant cleaning effect is associated with cavitation whereas this cavitation is suppressed under realistic downhole conditions, cleaning effects have still been detected. Micro streaming is a plausible explanation. It simply is a flow caused by wave propagation which creates drag forces that detach contaminants from in-situ rock and get mobilized with production flow.

A simple flow experiment on a mud cake damaged core was conducted to evaluated cleaning efficiency and regained permeability under different acoustic energy settings. They used an acoustic horn with a constant frequency of 20 kHz and a maximum power of 2000

Watt. Observations are made with varying acoustic burst durations, different flow conditions (static vs. flowing) and with different fluid pressures. Influences of temperature on fluid viscosity are corrected throughout all experiments.

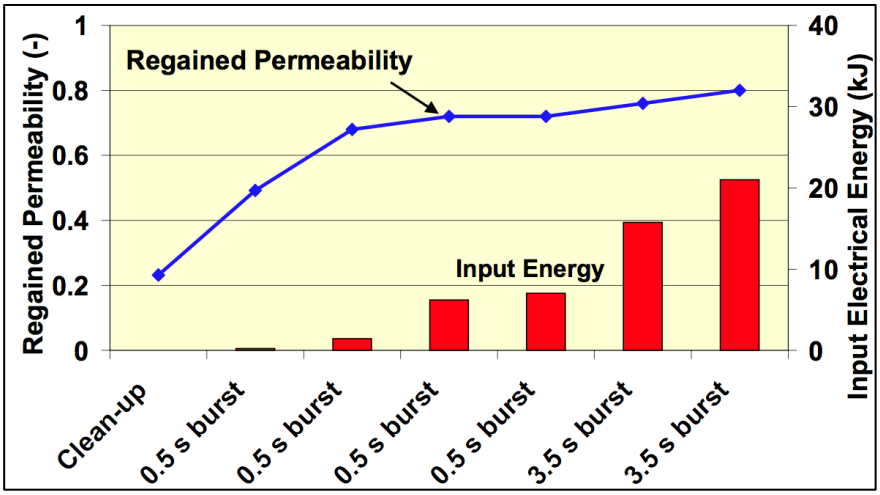


Figure 15: Regained permeability under acoustic stimulation with different input energies. [33, p. 3]

Results of the exposure time experiment showed that most of the cleaning is achieved directly after the signal is turned on resulting to an input electrical energy after 0.5 s of 2 kJ. The regained permeability yields up to 70% of the undamaged value. It finally reaches its maximum of 80% after 3.5 seconds corresponding to a 20 kJ power input as indicated in Figure 15.

Regarding results from acoustic treatment under static vs. flowing conditions, a regained permeability of only 50% is observed under no flow stimulation. Burst duration was 0.5 seconds yielding about 6 kJ energy input. Further acoustic bursts followed under flow conditions reaching a permeability of 80%. This confirms the feasibility of acoustic stimulation under static conditions, but with substantially higher energy requirements. A comparison of flowing and static conditions is presented in Figure 16.

When increasing the acoustic burst to 3.5 seconds corresponding to an energy input of 30 kJ no higher regained permeability could be reached. This fact consequently leads to the conclusion that tools capable of delivering short duration burst should be preferred.

Further observations were an overall increase in cleaning efficiency and cleaning rate with higher acoustic pressures and applied energy. At low fluid pressures cavitation can occur, thus needing a higher input electrical power to be able to create sufficient high acoustic power. Therefore, energy efficiency in downhole conditions at elevated pressures are superior as cavitation is suppressed and energy input can be reduced.

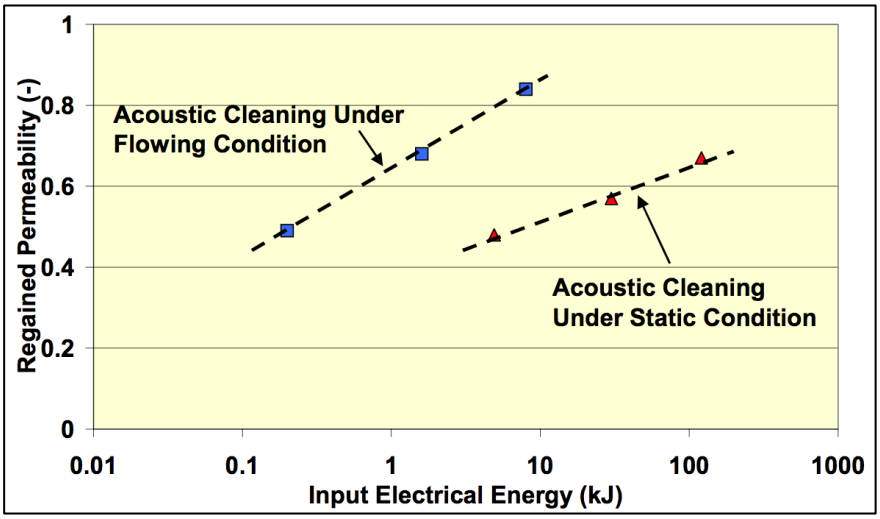


Figure 16: Comparison of energy requirements under flowing and static conditions. [33, p. 4]

With these findings, it was possible to transfer all influencing effects to a prototype downhole tool which works in oval-mode and propagates acoustic waves in radial direction. It can withstand downhole conditions and can be deployed with standard wireline cables, transmitting 2000 Watts. Unfortunately, no further information about on-field test were provided.

In a consecutive experiment Van der Bas et al. [5] used the previously developed radial acoustic stimulation prototype for further laboratory experiment. They used an acoustic horn which delivers an acoustic frequency of 20 kHz and a maximum power of 2000 W. The amplitude reaches 10 to 20 micrometers and can be boosted by a factor of two. Inside a thick-walled outer shell the tool consist of piezoelectric drivers and a pressure balance system rated to 1000 bar and temperatures up to 120°C. It is about 100 cm long and has a diameter of 7.4 cm. In operation, the outside wall of the tool is vibrated in an oval mode. The tool is concentrically inserted in a pressure vessel and can be moved axially and also rotation of 360° is possible. Hydrophones and accelerometers can be placed inside the cell to measure acoustic output power and get a clue about wave attenuation and depth of stimulation. A pressure drop along the core can be deducted and permeability can be back-calculated.

The main focus of the experiment was the removal of filter cake damage in a radial geometry. Therefore, a sintered wire-mesh screen was damaged with a mud cake and consequently treated with ultrasound. For comparison, a linear setup with the screen in front of a core sample is chosen. The mud cake is composed of a large range of calcium-carbonate particle sizes. For evaluation, the main parameter was the measured acoustic pressure as flow evaluations cannot be conducted. Influencing factors are frequency, voltage and fluid pressure inside the vessel. Further, a visual inspection of the screen was used for evaluation.

The linear acoustic clean-up treatment, which includes brine flow (2% KCl) and acoustic bursts, showed that the initial core permeability was completely regained and the mud cake was removed from the reservoir rock behind the screen. For comparison, conventional clean-up without ultrasonic excitation reach a permeability regain between 5% and 50%. That proves the feasibility of acoustic stimulation and removal of near wellbore damage under underbalanced pressure conditions. The radial experiment although being successful showed different results. The measured acoustic pressure was lower than in the linear experiment which resulted in an insufficient mud cake removal. In fact, it even seemed untouched at the surface of the screen. This is explained by the absence of flow and not enough energy input. Moreover, a 10% permeability decrease was observed during the acoustic stimulation. A possible explanation could be calcium carbonate particles released from the core due to excitation and plugging the screen. Promising indications were a mud spurt-loss after the acoustic treatment and when circulation continued. That indicates that the mud cake has been ruptured by excitation and not much more energy is required for a successful radial cleaning operation.

Further investigations to optimize the acoustic cleaning process were conducted by Van der Bas et al. [34] in a second publication. They used the same linear configuration as described in their previous papers [33] [5]. In addition, they examined the effectivity of acoustic cleaning of a mud cake from a reservoir rock in a gravel pack completion. Furthermore, an investigation of clean-up, flowing 100% light oil through an oil-based drilling fluid damaged core was conducted. Lastly, to simulate downhole conditions closely, experiments on a core containing oil at connate water saturation damaged with a water-based drill fluid were performed.

Results for the gravel pack experiment using 20/40 mesh sand in the annulus showed a permeability regain of 70% after 12 acoustic bursts each lasting for 0.5 seconds. Additional stimulation showed no effect. In the fully oil saturated core using light oil as displacement fluid acoustic cleaning granted a permeability regain between 80 and 90% showing similar results as brine displacement tests. Flow experiment at connate water saturation with a relative oil permeability of 0.9 showed a maximum regain of 60% which is relatively low compared to previous brine tests. This is explained by the decreased relative permeability due to water saturation and by reduced drag forces on the damaging particles. Also measured acoustic pressure showed a lower value due to different acoustic properties of oil and brine. Concerning all experimental outcomes, a concept for on field acoustic cleaning procedure has been developed. Most important is to stimulate the well under flowing/producing conditions with short subsequent acoustic bursts instead of continuous stimulation:

Main conclusion is that acoustic cleaning in oil is slightly less effective compared to brine cleaning.

An Austrian research team, Kunanz et al. [35], published test results using ultrasonic waves to remove scaling from the surface of a low grad steel half pipe which can represent the borehole or any other kind of pipe. Different scaling agents like calcium carbonate, gypsum/anhydrite or barium/strontium sulfate have a serious impact on productivity of oil and gas wells. Therefore, scaling prevention is a must have in modern operations. Chemical solutions used as scale inhibitor or scale dissolver are used so far. But their high costs and environmental impact make them inefficient and new technologies like ultrasound stimulation for cleaning purposes need to be understood and established.

Kunanz et al. performed laboratory experiments to verify ultrasonic cleaning efficiency on artificially generated gypsum scaling. Sonification was operated with a working frequency of 20 kHz with a maximum power of 2 kW. The contaminated steel pipe and the sonotrode were inserted in a water filled steel cylinder attached to a pump to simulate fluid flow. 24 experiments varying in flow or no flow, treatment time of 5 or 10 minutes and amplitude of 50 or 100% were conducted. Each sample was analyzed visually and gravimetrically, weighing the steel pipe with and without gypsum scaling and comparing it to the weight after ultrasonic treatment. The main parameter for comparison was the calculated purification factor.

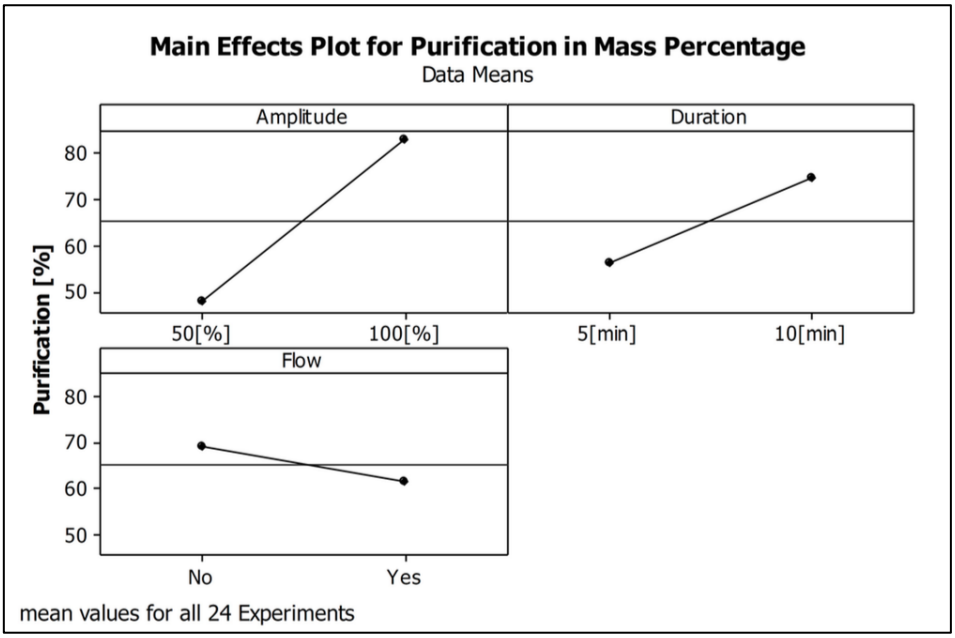


Figure 17: Main results from 24 ultrasonic cleaning experiments showing the major influencing parameters: amplitude, duration and flow conditions. [35, p. 8]

Results are shown in Figure 17. Basically, three parameters have the main effect on cleaning efficiency: an increase of vibration amplitude, which had the biggest impact, showed a higher purification; an increase in treatment duration also indicated better cleaning; the only

negative effect on purification occurred under flow conditions. Temperature rise did not automatically lead to a better cleaning effect.

Summarizing, the use of ultrasonic technology for cleaning purposes and for removing scaling from steel pipes proved to be feasible and is worth for further investigations.

### 2.1.4 Alteration of fluid properties

Experimental application of high frequency acoustic waves to investigate enhanced oil recovery often showed a decrease in fluid viscosity. It is not clarified if these changes have a thermal origin as heat is generated with the dissipation of ultrasonic energy or if other effects are responsible.

As viscosity plays a huge role in areal sweep efficiency, the effect of ultrasonic waves on the viscosity of different types of fluids is investigated by Hamidi et al. [36]. They used different ultrasonic frequency and power settings on paraffin, synthetic oil and kerosene, flowing in a capillary tube to evaluate changes in the pressure drop across the tube. Flow inside a capillary is assumed to be laminar and incompressible and therefore is Newtonian and can be defined with Poiseuilles's equation **eq. 14** [36, p. 2390]. Subsequently, fluid viscosity can be calculated.

$$\mu = \frac{\pi R^4 \Delta P}{2QL}\left(\frac{n}{3n+1}\right) \qquad (14)$$

$\Delta P$ Differential pressure [dynes/cm$^2$]
$L$ Length [cm]
$R$ Capillary radius [cm]
$\mu$ Liquid viscosity [poise]
$n$ Power-Law fluid index: $n = 1$
$Q$ Flow rate [cm$^3$/sec]

Experiments were performed under two different temperature conditions: uncontrolled and controlled temperature where excessive heat is withdrawn by a chiller. An evaluation of results shows the influence of temperature changes on viscosity. For both temperature conditions a reduction of viscosity was higher in lighter oleic fluids as it is easier to form cavitation in low density fluids. Further, the extend of the reduction is more significant in the uncontrolled temperature experiment. Hereby, the decrease of viscosity yielded 13%, 16% and 19% in respect to synthetic oil (17.29 API), paraffin oil (61.27 API) and kerosene (86.19 API). Whereas the increase under temperature control only reach 3.2%, 3.8% and 4.0%, respectively. For both experiments, ultrasonic frequency was set to 68 kHz and a power output of 500 W.

Further Hamidi et al. observed an additional viscosity decrease with increasing ultrasonic power, which again appears to be more effective in absence of temperature control as seen in Figure 18.

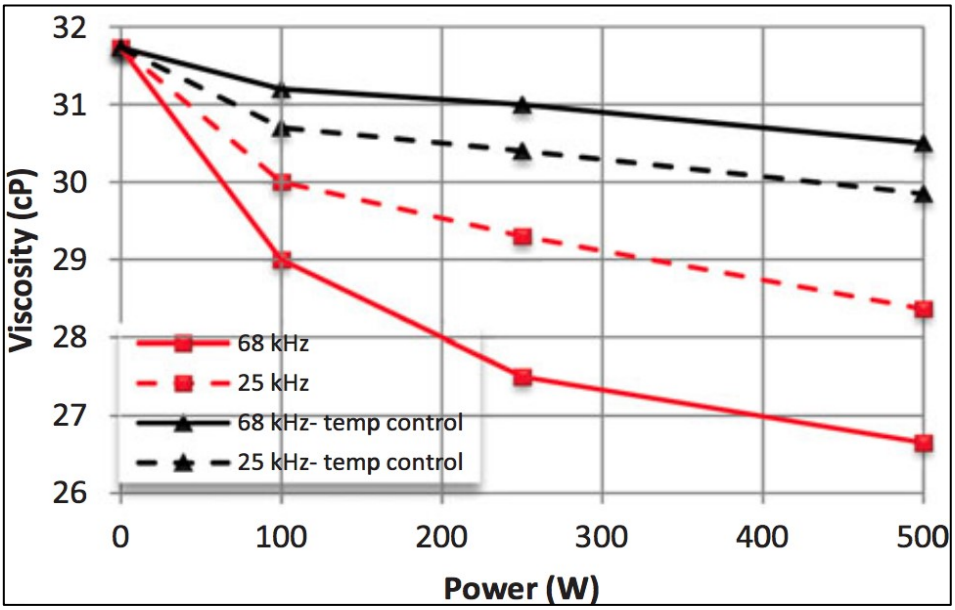


Figure 18: Changing paraffin oil viscosity under ultrasonic treatment. [36, p. 2393]

Concerning ultrasonic frequency, an increase causes a temperature rise induced by larger boundary friction at the interface of different media. Additionally, an increase of the amount of cavitation due to higher frequencies lead to a notable temperature rise. These two effects result in a reduced viscosity and can only be found under uncontrolled temperature conditions. With temperature control cavitation is most likely suppressed and no influence on viscosity can be determined.

Summarizing, the thermal effect on oleic fluids is the major influencing factor on viscosity. Although minor improvements can be detected when temperature effects are nullified proving an enhanced oil mobility under ultrasonic stimulation.

To investigate the effect of ultrasonic wave stimulation as an asphaltene flocculation inhibitor and consequently be able to reduce the actual asphaltene content of crude oils, Amani et al. [37] conducted an experimental study.

Asphaltenes can be part of crude oils and consist of large molecules of carbon, hydrogen nitrogen, etc. They can plug and damage the near wellbore region and restrict flow into the wellbore. Further they can accumulate inside pipes and other equipment and reduce the flow area until total blockage. To be able to reduce these effects with the help of ultrasound, sonication experiments (20 kHz and 1500 W power output), viscosity measurements, and asphaltenes extraction experiments were performed. Treatment time intervals were set to 2, 3, 5, 10, 15 and 20 minutes. After each ultrasonic treatment, asphaltene content was measured with an extraction experiment according to the America Society for Testing and Measurement (ASTM) D6560 (IP-143). The original asphaltene content of the crude oil before sonication was 3.20 wt.%. Until five minutes of excitation a decrease of asphaltene content was achieved reaching a minimum of 2.74 wt.%. This is explained by the

disintegration of the large asphaltic conglomerates into smaller particles and free radicals. As soon as sonication exceeds five minutes a gradual increase of asphaltene content was observed, which could be attributed to the formation of new particles due to the reintegration of the previously formed free radicals. This transition determines the optimum time for sonication (Figure 19), which is different for different crude samples according to their initial total asphaltenes content and their specific composition.

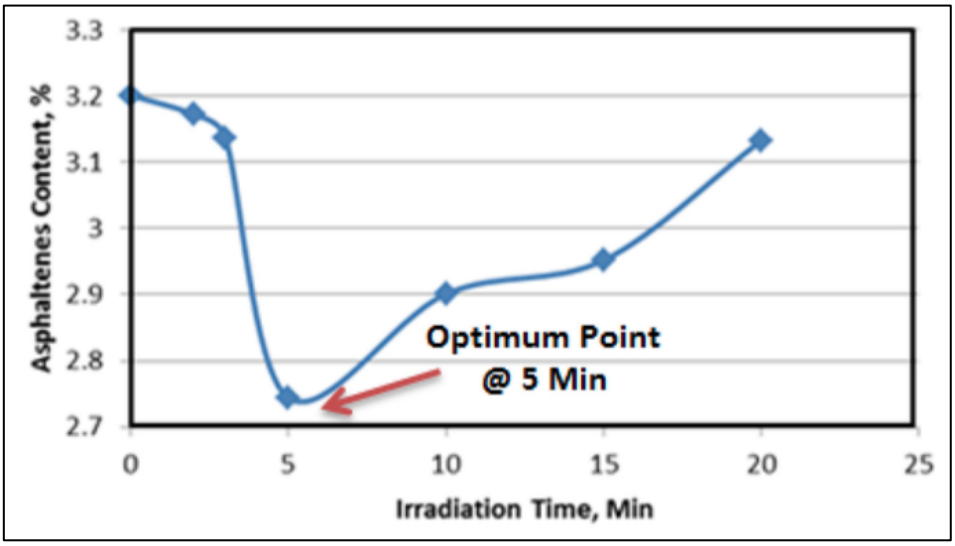


Figure 19: Asphaltenes content over acoustic treatment time. Optimum time for sonication is determined at 5 minutes. [37, p. 4]

Further, viscosity measurements indicted a strong dependency of viscosity to the asphaltenes content of the crude. In the beginning (<3 min) sonication increases viscosity as suspended particles get dissolute, which increases internal friction. Until the optimum point (5 min) a decrease of viscosity is achieved due to introduced heat when ultrasonic energy is dissipated as well as due to the disintegration of large asphaltenes flocs. After that, viscosity increases again caused by the integration of asphaltenes particles into long chain flocs.

Amani et al. conclude their research with the results that ultrasonic waves have the ability to break down asphaltenes conglomerates and be able to reduce asphaltenes content in crude oil samples. Hence, it proved to be an effective solution to asphaltene problems in the petroleum industry.

Tagiltcev and Korenbaum [38] analyzed the influence of ultrasound on the fluidity of heavy oil products under winter temperature conditions in pipes. The problem is the low fluidity of heavy oil under low temperatures (-15°C) when they become jelly-like. The aim is to decrease extreme starting loads on pumps of technological pipelines and secure transportation in crude oil pipelines.

Results showed a 20% fluidity increase found in the laboratory installation which was sonicated 20 seconds with a signal of about 25 kHz and an intensity of 0.002 W/cm$^2$. Reasons are the deformation of cubic skeleton of paraffin deposits and their liquefaction as well the rupture of long hydrocarbon chains due the intramolecular effect of ultrasound on hydrocarbon molecules.

The effect of ultrasound application during precipitation and crystallization processes is presented by Chen et al. [39]. They performed three sets of experiments: First, the crystallization of salt from a saturated solution as it cools down under ultrasonic excitation. Second, the dispersion of already formed asphaltene precipitates from a heptane suspension with ultrasound. Finally, pour point changes of diesel with different wax contents caused by ultrasound.

Ultrasound generation was magnetostrictive with a frequency of 20 kHz and 60 W power output. All solutions were heated up and then cooled down to simulate a wellbore environment during production, where thermodynamic changes can cause the solids to come out of solution and plug the well. Especially, in low rate producers with a constant laminar flow rate and very few turbulences, the occurrence of these precipitations is common as a “quiet” flow with low disturbances is needed for large crystals to form. Even slight agitation due to ultrasound can hinder the growth of crystals and prevent precipitations with all its consequences. To eliminate the effect of introduced heat due to ultrasound energy dissipation, temperature control was used during all experiments. Precipitated solids were observed under the microscope to determine their size. Results from treated samples with an ultrasonic disturbance and untreated samples were compared.

Results showed that the size of salt crystals can be reduced to a fraction of a millimeter with ultrasonic agitation. This promotes the adherence of the small crystals rather to suspended impurities in the produced fluid than to surface imperfections and therefore reduces precipitation. An extension of undisturbed flowing period of the well can be achieved.

The asphaltene experiments showed a change in the appearance of asphaltene precipitates under the microscope. It is assumed that ultrasound reduces the bonding between the aggregates and disperses flocculants. A long-term observation of the solution showed no further change of residues thus suggesting that the effect of ultrasound is irreversible.

The experiments on wax in diesel solutions showed the reduction in the pour point with the application of ultrasound. Results are summarized in Table 6.

Table 6: Change of pour point temperatures of different wax concentrations under ultrasonic agitation. [39, p. 5]

| ***Wax Concentration [wt%]*** | ***Pour Point no US [°C]*** | ***Pour Point with US [°C]*** | ***Δ°C*** |
|---|---|---|---|
| *10* | 19 | 1 | **18** |
| *20* | 25 | 14 | **11** |
| *30* | 29 | 22 | **7** |

That makes US a feasible tool to agitate individual crystals as they are coming out of solution so that they do not have a possibility to bond and preventing them to form large structures. This can prevent precipitations and prolong the life of a well.

As ultrasonic treatment on stationary samples during precipitation does not represent the real behavior in the field, Towler et al. [40] present experiments to measure the effect of ultrasonic waves on wax deposition during crude oil flow in a pipe. During the production of wax rich oils a decline of flow can be observed before the well gets totally plugged. This is due to the wax continuously dropping out of solution and precipitating on the wall of the tubing.

To be able to decompose the wax and inhibit it from deposition on the tubing, ultrasonic waves at a frequency of 120 kHz and a power of 50 W for each transducer are used. To introduce sufficient ultrasonic power, six piezoelectric transducers were mounted to the pipe. The main experiments were performed under laminar flow conditions with a flow rate of 1.1 gal/min, leading to a Reynolds number of 1815. The pipes were cooled from the outside letting the wax precipitate. After the treatment waxes were removed and compared to the deposits from the control experiment without ultrasonic agitation.

Unfortunately, ultrasonic waves only showed a minimal effect on the wax deposition. A slight decrease was observed with increasing temperature which is due to the heating effect of ultrasound dissipation which is also seen by the observed viscosity decrease. All in all, some reduction in wax deposition was achieved but it is in this case questionable if ultrasound technology is a feasible tool to treat wax under flow conditions. Further investigations with different ultrasonic frequencies and power outputs need to be done.

## 2.2 Hydrates

As this thesis concentrates on the effect of US on ice, which can be used as a substitute for natural gas hydrates, it is essential to understand the principles and the behavior of these hydrates.

In the petroleum industry, gas hydrates are substances that are usually gaseous at room temperature and under certain physical conditions (pressure and temperature) and in presence of water form crystalline solid compounds. They are a subset of clathrates or inclusion compounds and are similar in their physical behavior to normal ice. Their components are basically found in natural gas, which is a mixture of hydrocarbons such as methane, ethane, propane and a few nonhydrocarbons like hydrogen sulfide, carbon dioxide, nitrogen, and some more.

The formation of hydrates is one of the problems occurring during production, processing and transportation of natural gas. Incidents directly or indirectly associated with hydrates and their mishandling cost the natural gas industry millions of dollars. Even worse is the threatening of human lives due to accidents or improper operations. Therefore, the inhibition of hydrate formation and the effective removal of hydrate precipitations and plugs are a crucial task to understand and prompt constant improvement. [3]

### 2.2.1 Formation of Hydrates

Hydrates form due to the strong hydrogen bond of water that causes water molecules to align in regular orientations and be able to enclose small molecules. This forms a stable hydrate crystal. It has a complex, three-dimensional structure where the water molecules (“host” molecules) form a cage and the “guest” molecules (“formers”) are entrapped in these cages.

There are three interconnected conditions that have to be met individually to allow hydrates to form:

1. A proper temperature and pressure environment which variates with different compositions of hydrates must be met. In general, low temperatures and high pressures are required. These conditions are plotted in hydrate curves that map the region in the pressure–temperature plane where hydrates can form (Figure 20).
2. Hydrate formers like methane, ethane, carbon dioxide, etc. must be present.
3. An adequate amount of water must be available.

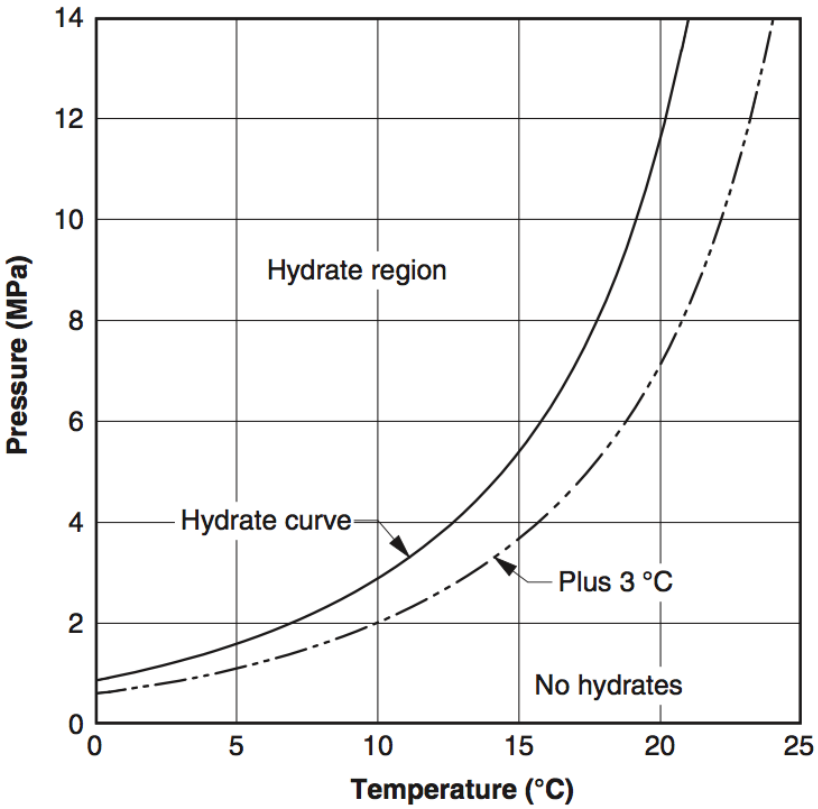


Figure 20: Hydrate curve showing the hydrate region. The region to the left and above (high pressure, low temperature) is where hydrates can form. In the region to the right and below hydrates cannot form. A safety margin is included and adds 3°C. [3, p. 14]

Other conditions can enhance hydrate formation but are not necessarily required:

1. Turbulence, including high fluid velocities and agitation. Especially at choke valves where first a temperature drop, due to expansion of natural gas (Joule-Thomson-Effect) happens. Second, fluid velocity increases through the restriction in the valve. Also, the mixing in pipelines and other surface equipment enhances hydrate formation.
2. Nucleation points where a phase transition is favored. These can be pipeline fittings, weld spots, imperfections or even solid particles from corrosion, scales or dirt. Also sand from gas production can be a nucleation site.
3. Free-water enhances hydrate formation and increases the probability of forming a plug.

Further, the accumulation side of the solid hydrate must be considered as it can differ from the point of formation. Hydrates can flow with the fluid stream and create a so called cold flow. In general, the accumulation of hydrates causes the problems and can block the line, plug and damage equipment.

### 2.2.2 Hydrate Types

Natural gas hydrates are categorized according to the crystal structure induced by the arrangement of water molecules. In the petroleum industry two polyhedral types of hydrates are commonly found: type I and type II. As type H is rarely encountered it will not be discussed in this thesis.

#### 2.2.2.1 Type I Hydrates

Type I hydrates with the simplest structure can either have a

a) dodecahedron structure with a 12-sided polyhedron where each face is a regular pentagon
b) tetrakaidecahedron structure with a 14-sided polyhedron with 12 pentagonal faces and 2 hexagonal faces (Figure 21).

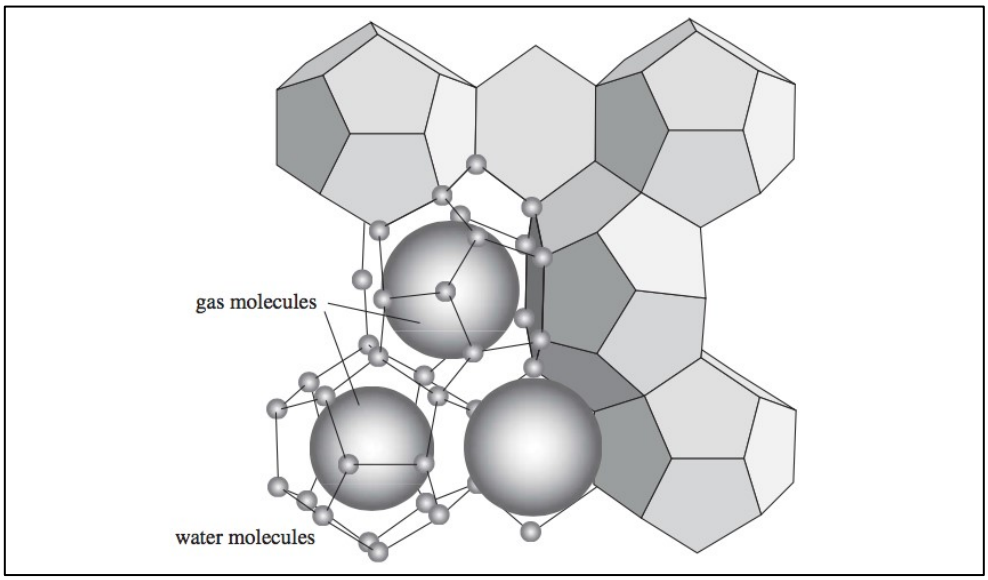


Figure 21: Type I Hydrate with a 14-sided polyhedron with 12 pentagonal faces and 2 hexagonal faces. [41, p. 2371]

Type I cages can enclose gas molecules that are smaller in diameter than propane molecules, such as methane, carbon dioxide or hydrogen sulfide. They consist of 46 water molecules and the theoretical formula is $X \cdot 5\,{}^{3}/_{4}\,H_2O$, where X is the hydrate former.

#### 2.2.2.2 Type II Hydrates

Type II is significantly more complicated and contains gases with molecules larger than ethane and smaller than pentane such as nitrogen, propane and isobutane. There are also two types of structures:

a) dodecahedron structure with a 12-sided polyhedron where each face is a regular pentagon
b) hex- akaidecahedron structure with a 16-sided polyhedron with 12 pentagonal faces and 4 hexagonal faces.

Type II hydrate consists of 136 molecules of water and the theoretical formula is $X \cdot {}^{2}/_{3}\, H_2O$.

### 2.2.3 Inhibition of Hydrate Formation

The basic way to prevent hydrate formation is to eliminate one of the three formation conditions discussed earlier. Two of them are feasible as we cannot remove hydrate formers as these are the desired products. So, attacking pressure and temperature conditions and/or removing water from the mixture is the most reasonable approach.

To increase the threshold of hydrate forming temperature the most common method is to use chemicals such as methanol, ethylene glycol (EG) or triethylene glycol (TEG). These solutes use the depression of the freezing point of a solvent. In Figure 22 the effect of different chemicals on hydrate forming temperature is shown.

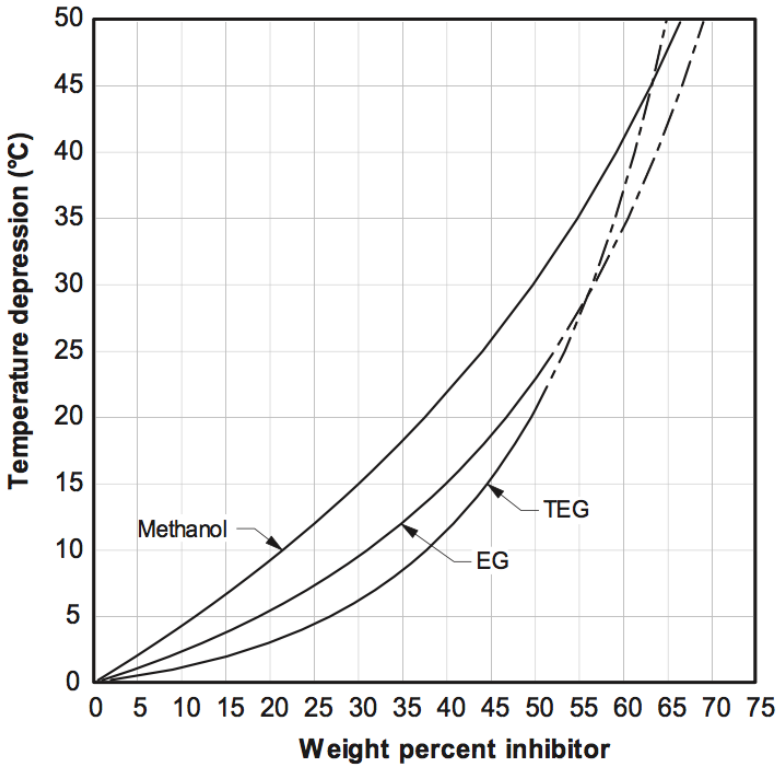


Figure 22: Temperature depression and hydrate inhibition of methanol, ethylene glycol (EG) and triethylene glycol (TEG). [3, p. 143]

Even though methanol is very effective as a hydrate inhibitor in pipelines and process equipment, it has some undesirable side effects:

1. Processing products such as LPG can have unacceptable amounts of methanol, which cannot be removed from the hydrocarbon stream.
2. It can dissolve corrosion inhibitors, which are injected at the same time. This could lead to severe corrosion problems.
3. Another potential problem related to methanol injection is due to the dissolved air in the methanol, which is responsible for additional corrosion.
4. Methanol is used as a fuel and has a high flammability. From a fire prevention point of view, the storage is considerable dangerous and the fire hazard is significant.
5. Methanol is toxic when consumed in large enough quantities. The lethal dose is 1-2 ml/kg body weight. [42]
6. Methanol is fairly cheap but usually it is not recovered and reused such as glycol.

Glycol is much more cost effective but also has adverse effects:

1. As well it is flammable but to a lower degree as methanol.
2. It is toxic and its lethal dose is about 1.4 ml/kg of body weight. [43]
3. Glycols have a sweet flavor, which is attractive to children and some animals.
4. The cost of glycol is significantly greater than methanol.

On the other hand, there are hydrate inhibitors that are not working thermodynamically. These are so called low dosage inhibitors and are either kinetic inhibitors or anticogualants. These types are not commonly found in the industry as they are quite new and still expensive. Kinetic inhibitors delay hydrate formation and growth but do not prevent the hydrate from crystallizing. Anticogualant do not prevent hydrate formation but its accumulation into plugs as the hydrate stays in a slurry.

To eliminate the third formation condition, water has to be removed from natural gas. Dehydration processes are common methods for preventing hydrate formation. There are several methods of dehydrating natural gas:

1. glycol dehydration (liquid drying agent - absorption)
2. molecular sieves (solid adsorbent - adsorption)
3. refrigeration (condensation)

### 2.2.4 Hydrate Removal

In many cases hydrates form but flow with the fluid in the line causing only minimal flow problems. But if they accumulate and form a plug, hydrates cause a severe safety hazard and have to be removed immediately. First signs of hydrate accumulation are related with an increase in pressure drop due to a flow restriction and show a rising trend as the plug quickly changes in size. Ultimately, the plug is formed and causes a dramatically increased pressure drop. An important consideration is that in many cases not only a single hydrate plug is

formed but a high possibility exists that multiple plugs blocking the line. There are several hydrate remediation techniques available:

1. Depressurization in means of reducing the line pressure below the hydrate formation pressure causing the hydrate to become thermodynamically unstable. This process though doesn't work instantaneously as the plug will melt radially inward and detaches first at the pipe wall. This causes a potential safety hazard when the pressure is only reduced at one side of the plug. It will lead to a large pressure gradient across the plug and can form a hydrate projectile erupting from the pipe and destroying surface equipment.
2. Adding heat to the system or using heat tracing is another method. This active heating causes the temperature to rise above the hydrate dissociation temperature and melts the hydrate. Heat tracing can be either electrical or by a fluid and is placed adjacent to the line that is to be heated. It is especially useful on valves as these are prone to freeze due to the Joule-Thomson effect. Compared to depressurization, which can take days to remediate the blockage, active heating can melt large plugs in hours. However, this method should also be used with caution. During the disintegration process, huge amounts of gas and liquid water are released from the plug. If the gas is trapped, pressure can build up tremendously and is capable of rupturing most flowlines.
3. Increasing the injection rate of thermodynamic inhibitors such as methanol, ethylene glycol (EG) or triethylene glycol (TEG) can essentially melt blockages with direct hydrate contact. This Method may not always help with dissociating a hydrate blockage but prevent more to accumulate.
4. Mechanical methods such as drilling, pigging, and scraping have been attempted, but are generally not recommended. Using coiled tubing to free the hydrate plug by removing liquid hydrostatic head at the hydrate face to enhance depressurization or jetting inhibitor directly at the hydrate, are more viable operations.
5. An ultimate measure would be to replace the plugged section of the pipe.

Using ultrasonic waves to dissolve and destroy hydrate plugs in surface pipelines is a very new technology that still has to be validated in the future. But as it is the main objective of this thesis one thing ahead: first experiments showed promising results.

### 2.2.5 Physical Properties of Hydrates

Physical properties are important for understanding the behavior of hydrates and consequently making good decisions in planning inhibition and/or removal operations. Most of the properties of hydrates like heat capacity, electrical, and mechanical properties are similar to those of ice. Therefore, it is viable to substitute hydrates with ice for our laboratory experiments. Table 7 shows a variety of physical properties comparing some hydrates, ice and water at 25°C. Concerning mechanical properties, the assumption can be made that those of most hydrates equal those of ice and can form very hard blocks. A key property that differentiates ice from hydrates is the thermal conductivity. It is with 0.50 W/mK significantly

lower than ice (2.2 W/mK). This relative small value explains why hydrates take such a long time to melt. [44]

Table 7: Physical properties of some hydrates, ice and water. [45] [46] [47]

| ***Hydrate*** | ***Hydrate Type*** | ***Molar Mass [g/mol]*** | ***Density [g/cm$^3$]*** | ***Enthalpy of Fusion [kJ/g]*** | ***Heat Capacity [J/g°C]*** |
|---|---|---|---|---|---|
| *Methane* | I | 17.74 | 0.913 | 3.06 | 2.25 |
| *Ethane* | I | 19.39 | 0.967 | 3.70 | 2.2 |
| *Propane* | II | 19.46 | 0.899 | 6.64 | 2.2 |
| *Isobutane* | II | 20.24 | 0.934 | 6.58 | 2.2 |
| *$CO_2$* | I | 21.59 | 1.107 | 0.5 | 2.08 |
| *$H_2S$* | I | 20.87 | 1.046 | - | - |
| *Ice* | - | 18.01 | 0.917 | 0.33 | 2.06 |
| *Water* | - | 18.01 | 1.000 | 2.83 | 4.18 |

# 3 Practical Work & Laboratory Experiment

In this chapter, all different experiments dealing with the behavior of ice under ultrasonic excitation are explained. Three different setups to evaluate the feasibility will be described and analyzed. All used equipment and detailed overviews of the setups are shown. Setup 1 was used the get first insights of the impact of ultrasonic waves on ice; therefore, a simple household ultrasonic cleaner with a basic setup is used. Setup 2 compares the duration of ice plug removal in a prototype steel cylinder. The main focus lies on Setup 3, as pressure sensors are used to get ideas about the temporal dissolution of the plug under pressure and the influence of changing ultrasonic fields. Plug breakthrough times are evaluated and compared. Dissolved volume is monitored and assessed.

## 3.1 Assumptions and Expectations

As mentioned in the previous chapter, ice has very similar properties compared to those of hydrates. Therefore, ice acted as a substitute and replaced natural gas hydrates in the laboratory experiment. Reasons for that are firstly, hydrates are very complicated to produce artificially, secondly, hydrates are unstable under ambient conditions and can be very dangerous to handle, and thirdly, ice is a convenient, cheap and physically feasible choice.

Using ultrasonic waves to dissolve and destroy hydrate plugs in surface pipelines and equipment is a very new technology that still has to be validated. The idea is to change the position of the ultrasonic transducer from inside of the pipe, where ultrasonic waves are in direct contact to the plugging medium, to the outside of the steel body. The steel wall then should act as an additional transmitter of ultrasonic waves and should disperse the energy evenly around the pipe, leading to an efficient dissolution of the hydrate plug starting at the inside wall of the pipe. Consequently, as the plugging material gets detached from the surface, the plug gets mobile and can be removed at the next access point, for example a filter station. In addition, mechanical vibration due to the ultrasonic excitation are believed to disintegrate the hydrate plug which could lead to an easy to handle cold flow.

Another supporting effect to dissolve the ice plug is the heat which is introduced by the energy of the ultrasonic wave and its generation in the piezoelectric transducer. The ultrasonic energy is dissipated by ice consequently lowering the overall system temperature, which is one major formation factor governing the stability of the hydrate.

The effect of high pressures on the abundance and the power of cavitation, which is believed to aid the dissolution, is already mentioned in the fundamentals section. Therefore, experiments under different pressure levels are compared. Further, the effects of different levels of ultrasonic energy input is analyzed. It is assumed that a higher energy input will lead to faster dissolution of the plug and a more severe disintegration of the ice.

## 3.2 Equipment and Setup

In this section, all the equipment utilized for the three setups during the laboratory experiment is listed.

### 3.2.1 Setup 1 – Household ultrasonic cleaner

#### 3.2.1.1 GT SONIC-F1

The main purpose of the GT Sonic-F1 household ultrasonic cleaning machine (Figure 23) focuses on cleaning, disinfection and sterilization of daily necessities such as eyeglasses and jewelry. Its specifications are summarized in Table 8. It consists of a 600 ml oval-shaped steel tank to which one high-power ultrasonic transducer is mounted. The transducer has the shape of a piezoceramic disc and operates with a fixed working frequency of 40 kHz and a power output of 35 W, which is enough for mild but effective treatment. The generation of ultrasonic waves is based on the reverse piezoelectric effect and hence the working frequency cannot be adjusted, because it is given by the piezoelectric material used in the transducer. Also, the amplitude of the ultrasonic wave cannot be adjusted, as the generator is built in and is very simple in design. The device is operated with a single on/off button, which starts a timed sonication of five minutes. The cleaner can also be switched off manually after a desired time.


Figure 23: GT Sonic-F1 ultrasonic cleaner. [48]

Table 8: Specifications of household ultrasonic cleaner GT Sonic-F1 [48]

| ***Model*** | ***GT Sonic-F1*** |
|---|---|
| *Ultrasonic Frequency* | 40 kHz |
| *Tank Material* | Stainless Steel SUS304 |
| *Tank Capacity* | 600 ml |
| *Timer* | 5 min |
| *Power Supply* | AC 100~120 V, 60 Hz; AC 220~240V, 50 Hz |
| *Ultrasonic Power* | 35 W |
| *Tank Size* | 154x94x46 (l×w×h) (mm) |
| *Overall Size* | 209x200x121 (l×w×h) (mm) |

### 3.2.2 Setup 2 – Duration of ice plug dissolution

#### 3.2.2.1 Steel Cylinder

For all further experiments a prototype steel cylinder is used and modified to act as an ultrasonic cleaning chamber (Figure 24). It has a fixed closed bottom, an open top which can be sealed with a blind flange and suitable gaskets (Figure 25), an inlet at the bottom and an outlet at the top. Its dimensions are shown in Figure 24. The wall thickness is 5 mm. The material is a 304L stainless steel which is comparable to a 18-8 CrNi steel.

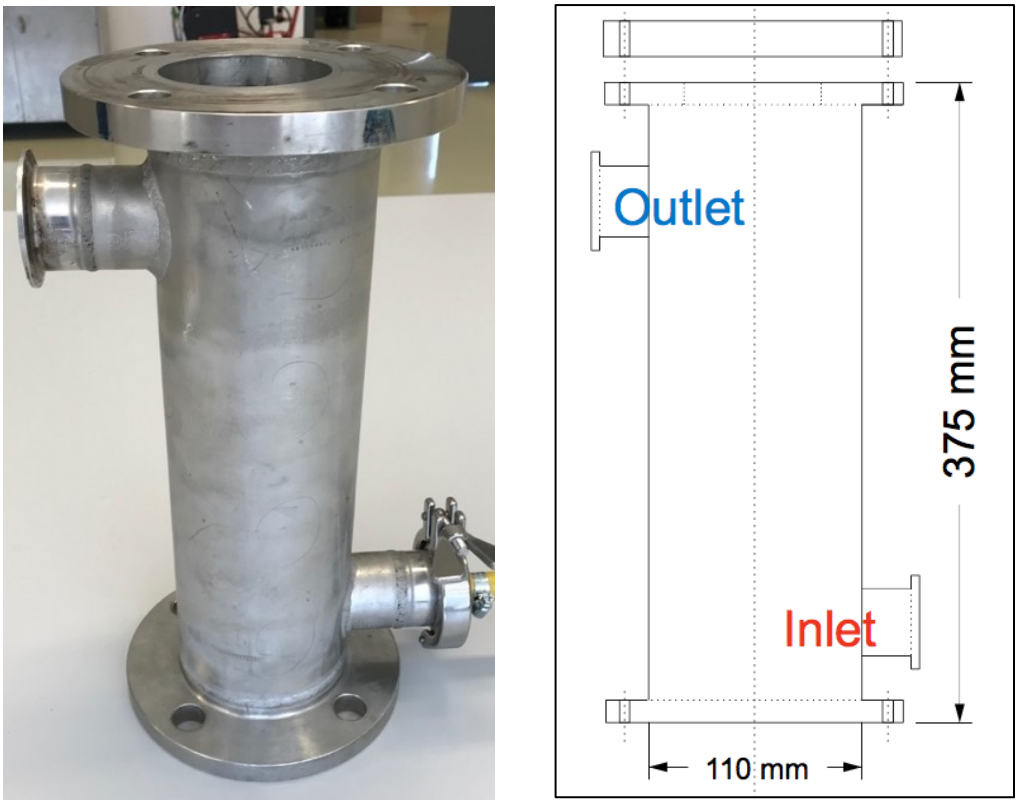


Figure 24: Prototype Steel Cylinder witch dimensions.

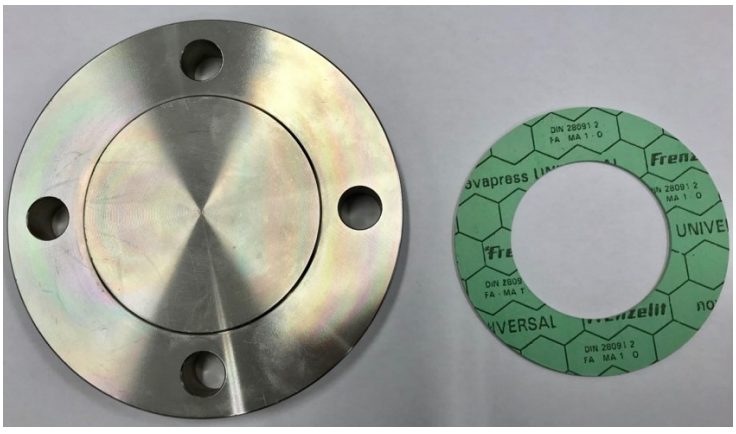

Figure 25: Blind flange and gasket: ASME Class 150 B 16.5 2½”

### 3.2.2.2 Ultrasonic Transducers from “UCE Ultrasonics”

To convert electrical energy from the ultrasonic generator into mechanical oscillations to be applied on the outside of the steel cylinder, multiple ultrasonic transducer from “UCE Ultrasonics” are used (Figure 26). Their specifications are shown in Table 9. The resonant frequency of each transducer is 25 kHz; the maximum effective power is 100 W. The topmost part of the transducer, the so called “sonotrode” or “vibration head” is responsible for the transportation of the vibration from the transducer onto the steel cylinder. The horn like shape of the sonotrode generates a broad wave field which is best suited for cleaning operations. The transduction efficiency between the high frequency high power electrical signal and the mechanical sound wave is 95% according to the producer.

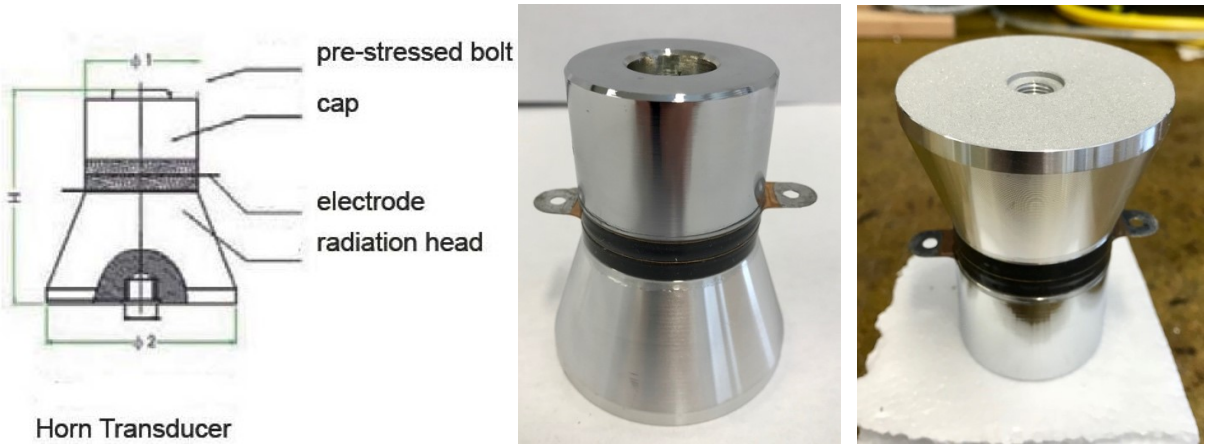


Figure 26: Horn shaped ultrasonic transducers: UCE-UT-25100 PZT-4

Table 9: Specifications of ultrasonic transducer UCE-UT-25100 PZT-4. [49]

| ***Model*** | ***Transducer UCE-UT-25100 PZT-4*** |
|---|---|
| *Ultrasonic Frequency* | 25 kHz |
| *Max. Input Power* | 100 W |
| *Length (L)* | 77 mm |
| *Diameter 1 (∅1)* | 44 mm |
| *Diameter 2 (∅2)* | 67 mm |
| *Weight* | 710 g |
| *Resonant Impedance* | 10 – 20 Ω |
| *Static Capacity* | 6600 pF |

#### 3.2.2.3 Ultrasonic Generator from “UCE Ultrasonics”

The “UCE-NT2500” ultrasonic generator (Figure 27) with automatic frequency adjustment works in the range of 19 – 43 kHz and adjusts the resonant frequency automatically. The power output of the device is maximum 2500 W. Consequently, a maximum of 25 ultrasonic transducers (UCE-UT-25100 PZT-4) can be driven simultaneously. The power can be adjusted between 0 – 100% in 16 steps. The generator is able to perform a sweep mode to simulate a scouring effect by regularly changing the bandwidth of the frequency. The display can show actual frequency in kHz, signal amplitude in ampere and the elapsed sonication time. All specifications are shown in Table 10. A full electric scheme is presented in Appendix A.

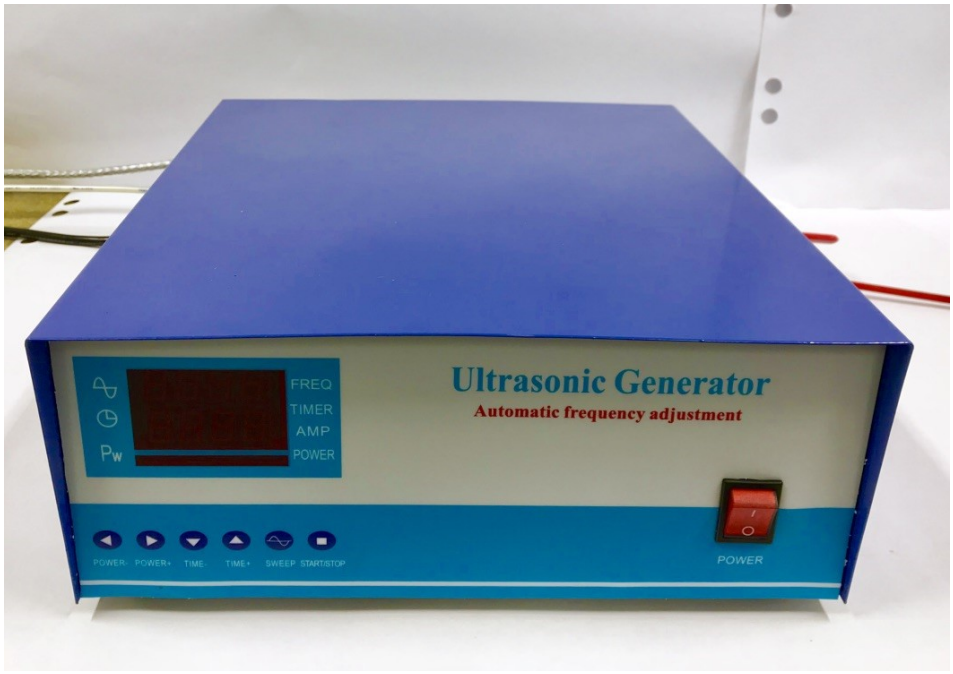


Figure 27: 2500 W Ultrasonic generator: UCE-NT2500.

Table 10: Specifications of ultrasonic generator UCE-NT2500. [50]

| ***Model*** | ***Transducer UCE-UT-25100 PZT-4*** |
|---|---|
| *Ultrasonic Frequency* | 25 kHz; adjustable 19-43 kHz |
| *Max. Output Power* | 2500 W |
| *Power Supply* | AC 220-240V, 50 Hz |
| *Max. Current (Amplitude)* | 8.5 A |
| *Power Control* | 0 - 100%; 16 Levels |
| *Sweep Mode* | Yes |
| *Timer* | 0 - 59 min |
| *Size* | 300x360x150 mm (l x w x h) |

To be able to drive multiple transducers with the same frequency and power simultaneously, all transducers must be wired in a parallel circuit. A shielded cable is used to connect the generator with the transducers. The applied electronic schematic is shown in Figure 28.

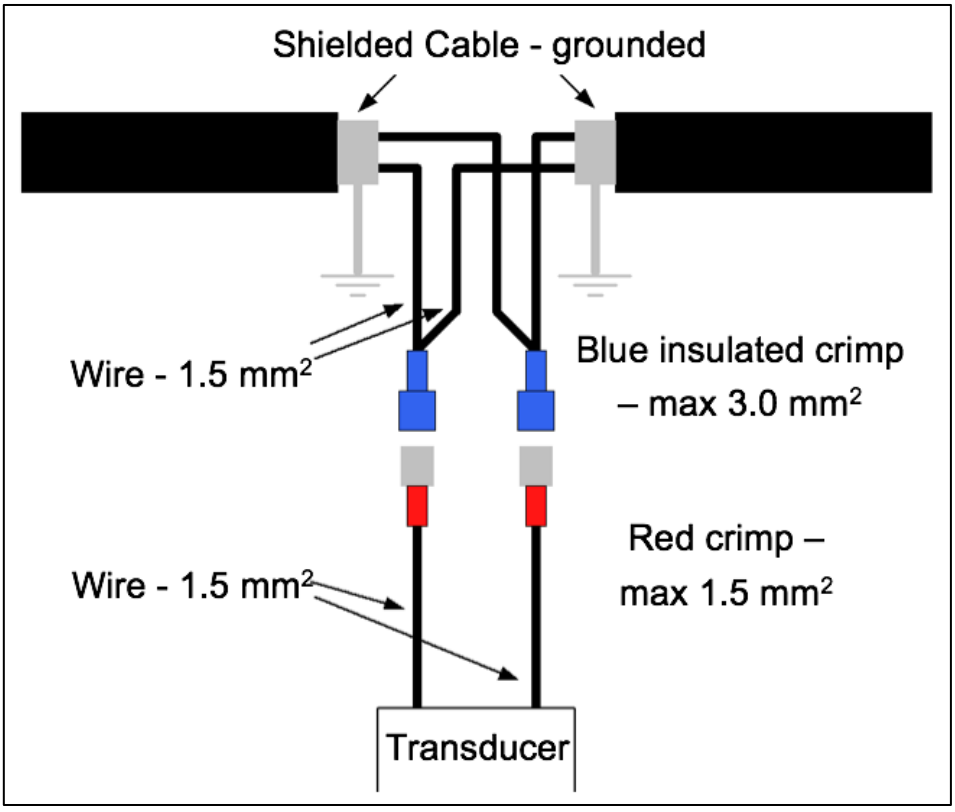


Figure 28: Electronic schematic of a parallel connection of multiple transducers.

#### 3.2.2.4 Bosch GSN 58 AW Freezer

A Bosch GSN 58 AW freezer was used to freeze the steel cylinder filled with 3000 ml water to create an ice plug clogging a flowline. The temperature of the freezer was set to a constant -24°C.

#### 3.2.2.5 Metal Loaded Epoxy Glue “RS Pro 850-962”

To be able to attach the ultrasonic transducers onto the steel cylinder a two-component metal loaded epoxy glue is used (Figure 29). Its properties are shown in Table 11. The advantage of the epoxy is that it gels within 5 minutes after mixing and forms a strong bond to most metal surfaces, filling gaps and holes. It reaches full strength after 24 hours. It is not flexible and has a very high shear strength, hence being perfect for transmitting ultrasonic waves.


Figure 29: 25 ml twin syringe of metal filled epoxy glue.

Table 11: Specification of Epoxy Glue.

| ***Model*** | ***Epoxy Glue RS Pro 850-962*** |
|---|---|
| *Material compatibility* | Metal |
| *Setting Time* | 5 min |
| *Cure Time* | 24 h |
| *Filler Material* | Inorganic: Magnetite |
| *Chemical Composition* | Barium Sulphate, Bisphenol A-(Epichlorhydrin), Limestone, Magnesium Carbonate, Talc |

### 3.2.3 Setup 3 – Pressure breakthrough time of a plugged steel cylinder

In addition to the equipment used in Setup 2 following devices are used.

#### 3.2.3.1 Pressure Gauge “Testo 549i”

Two Testo 549i high-pressure measuring instruments (Figure 30) are connected directly to the pressurized line; one at the inlet of the cylinder and the other to the outlet, respectively. The gauges can be connected via Bluetooth to a smartphone or a tablet and are controlled via the Testo Smart Probes App. All measured data can be displayed either as a chart or in table form and be send to an e-mail address for further processing. The range of measurement is from -1 to +60 bar, the resolution is 0.01 bar and the operating temperature is between -20 and +50°C. It can handle different pressure media such as air, nitrogen, carbon dioxide, and all types of liquids such as water.


Figure 30: Testo 549i - high-pressure measuring instrument with smartphone operation.[51]

### 3.2.3.2 Pressure Pump “Swissnox Typ MEDI”

A simple hand operated pressure pump (Figure 31) is used to pressurize the system. A maximum pressure of 15 bar is applied to the steel cylinder. As pressure medium, normal tap water is used. The pressure connections to and away from the cylinder are realized with polyamide-hoses with an outer diameter of 5 mm. A couple of different connectors, adapters and valves are used.


Figure 31: Pressure Pump “Swissnox Typ MEDI”.

## 3.3 Laboratory Experiment

### 3.3.1 Setup 1 – Household ultrasonic cleaner

To get first insights of the impact of ultrasonic waves on ice, a simple household ultrasonic cleaner with a basic setup is used. Overall five experiments were conducted. Changing parameters are the fluid type, which was either tap water or distilled water and sonication time, which varies between 10 and 60 minutes. The procedure stayed the same throughout this set of experiments:

First, the ultrasonic cleaner is disassembled as shown in Figure 32. The bottom part, which contains the electrical components of the generator is disconnected from the steel tank, to which the piezo element is glued with epoxy resin. This is done to protect the delicate electrical components from freezing temperatures. The piezo crystal can easily withstand extreme colds but has major problems when temperature rises above 100°C as the crystal can be destroyed.

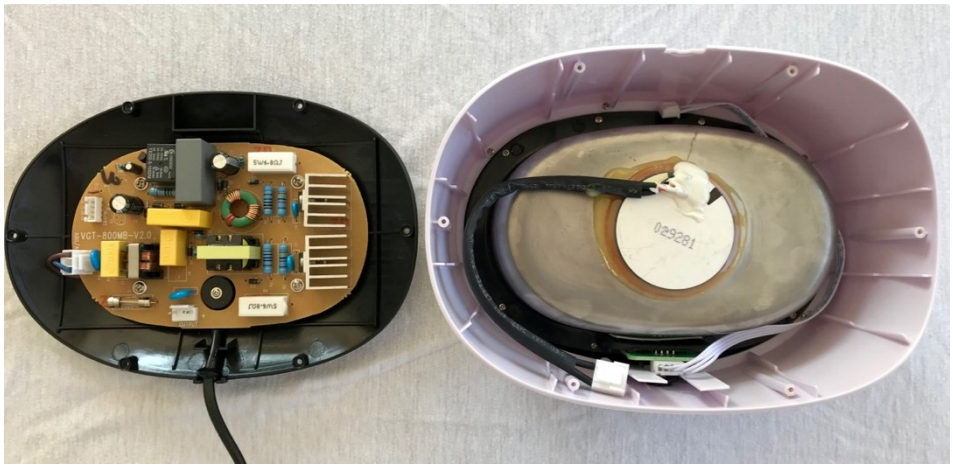

Figure 32: Disassembled household ultrasonic cleaner.

Then the steel tank is filled with 500 ml of either water or distilled water and frozen at -18°C for 24 hours. The result is a solid, partly cloudy ice block that is fixed in place and cannot be removed from the tank. Some minor fractures and frozen air bubbles are visible as shown in Figure 33. Subsequently, the ultrasonic cleaner is reassembled and switched on. After every five minutes of ultrasonic excitation, the ice block is examined and changes are documented. Further, the volume of dissolved water is measured and removed from the steel tank. In the end of the experiment the block of ice is removed from the tank, photos are taken and impacts of ultrasound are compared. Results can be found in the next chapter.

Figure 33: Frozen water inside a household ultrasonic cleaner before ultrasonic excitation.

### 3.3.2 Setup 2 – Duration of ice plug dissolution

Figure 34 shows the main setup, which generally is valid for Setup 2 and Setup 3. A graphical representation is found in Appendix B. On the left side, the ultrasonic generator “UCE-NT2500” is located. It is driven with the laboratory’s power grid and can be connected with shielded cables to a variable number of ultrasonic transducers. In the middle, the prototype steel cylinder is placed. Its inlet to the right is connected to the pressure line from the pressure pump. At this point, high pressure can be applied to the cylinder. The outlet to the left is connected to the pressure line which can be closed with a ball valve to be able to monitor pressure rises as soon as a communication between inlet and outlet is granted. In open stage, the pressure line leads to a disposal tank to be able to safely release pressures from the cylinder. The pressure pump far right is filled with normal tap water.


Figure 34: Main setup of the laboratory experiment.

During the experiment of Setup 2 all pressure lines and the steel cylinder are in open position as the whole system is unpressurized. First, the steel cylinder is cleaned and filled to the top with 3000 ml of tap water. It is then put in the freezer to stay there for 24 hours. Water freezes and creates a solid ice block that plugs the cylinder. As volume increases during the freezing process, excessive ice is removed before the experiment can begin. In the control experiment, the cylinder was completely left untouched for 8 hours. The only measurement taken regularly was the temperature from the steel cylinder at the inlet and the outlet. At the end of the experiment molten volume was removed. The value was than extrapolated to reach the initial 3000 ml to get the time for total dissolution of the ice plug under ambient conditions. Total dissolution time and a temperature curve are the results.

These values are then compared to those, when the cylinder is under ultrasonic excitation. Experiments are conducted with 2, 4 and 10 transducers, corresponding to a power output of 200, 400 and 1000 W, respectively. Results are presented in the next chapter.

Figure 35: Steel cylinder after 0, 5 and 40 minutes of ultrasonic excitation.

### 3.3.3 Setup 3 – Pressure breakthrough time of a plugged steel cylinder

The most evaluated experiment, Setup 3 was performed 11 times. Five times without any ultrasonic excitation and two times each for 2, 4 and 10 transducers switched on. Parameters including pressure breakthrough time, inlet temperature, outlet temperature, delta p inside the cylinder acting as resistance to free flow due to the ice block, resonant frequency, amplitude of the ultrasound signal and transducer temperature are gathered and compared. Results can be found in the next chapter.

The experimental procedure is similar to Setup 2. First, the steel cylinder is cleaned and filled to the top with 3000 ml of tap water. It is then put in the freezer to stay there for at least 24 hours. Water freezes and creates a solid ice block that plugs the cylinder. As volume increases during the freezing process, excessive ice has to be removed before the experiment can begin. The cylinder is tightly closed with a blind flange and a suitable gasket. The valve at the outlet pressure line is closed to immediately see any pressure changes. An initial pressure of about 12 – 14 bar is applied to the inlet of the cylinder.

During the set of non-ultrasonic experiments the cylinder is left alone until the ice blockage breaks and the pressure at inlet reaches the outlet, granting communication between those two. Every five minutes the temperature at inlet and outlet are measured to get a temperature profile. After the pressures at inlet and outlet are equalized all valves are opened and the pressure is released. Then a circulation through the cylinder is simulated by pumping water continuously for one minute. The average pressure difference between inlet and outlet is calculated and interpreted as the resistance to free flow inside the cylinder due to the block of ice. After 50 minutes the cylinder is opened, all molten volume is removed and measured and the experiment is completed.

During the set of experiments with ultrasonic excitation, the ultrasonic signal is switched on after the initial pressure is applied. Aside of temperature measurements every 5 minutes the frequency and amplitude of the generated ultrasound signal is monitored as well as the average transducer temperature. After the pressure breakthrough time the same procedure as in the non-ultrasonic experiment is performed. After 50 minutes the ultrasonic signal is turned off, molten volume is removed and the experiment is completed.

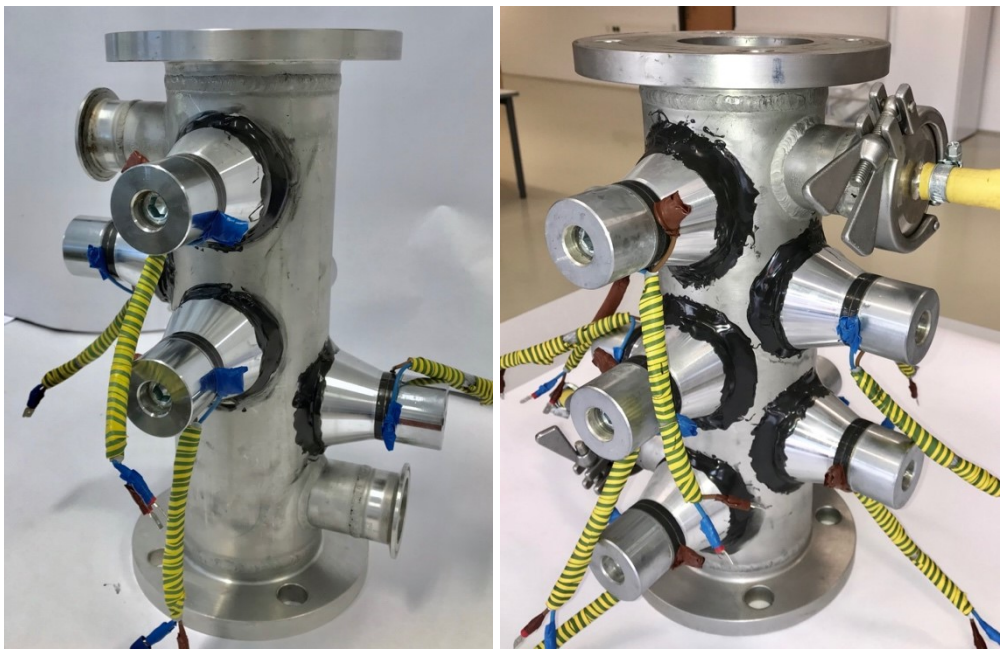

Figure 36: Ultrasonic cleaning cylinder with five transducers (left) and ten transducers (right).

# 4 Results

In this chapter, results are discussed separately for each experimental setup. An overall summary and personal recommendations can be found in the conclusion chapter.

## 4.1 Setup 1 – Household ultrasonic cleaner

All five experiments demonstrate the feasibility of ultrasonic excitation on ice. Further, all tests show a clear impact on the disintegration of the ice. Results are comparable and reproducible throughout Setup 1. Therefore, only one experimental test is visualized at this point.

Immediately after the ultrasonic cleaner is switched on, the influence of ultrasound is visually and acoustically perceptible. Small air bubbles as a result of ultrasonic cavitation emerge at certain spots inside the block of ice. The impact especially is visible directly above the ultrasonic transducer in the middle and at the contact area to the steel surface. Figure 37 shows the ice inside the cleaner after four seconds of treatment. Red circles indicate dissolution and cavitation effects.

Figure 37: Block of ice after 4 seconds of ultrasonic excitation. Red circles indicate air bubbles due to cavitation effects.

After 20 seconds of excitation the ice block cracks under the ultrasonic energy and a fracture alongside a big bubble in the middle appears (Figure 38). After five minutes the bubble has a size of about 1.5 cm in diameter. About 30 ml of water are dissolved at the contact area to the steel surface and removed from the tank. After 10 minutes, the ultrasonic signal is switched off to be able to remove the ice block. Additional 20 ml of water are removed. The block of ice appears to be very brittle at the bottom, where it is in direct contact to the

vibrating steel surface. Ice is molten in the shape of blocky breakouts at the edges as seen in Figure 39.

Figure 38: Block of ice after 20 seconds of ultrasonic excitation. To the left: a large fracture; in the middle: growing air bubble.

Figure 39: Ice after 10 minutes of ultrasonic excitation. Ice disintegrates in form of blocky breakouts. Very brittle at the bottom.

The block is put back into the cleaner and treated with US for additional 10 minutes. After the final excitation, 70 ml of water are removed which adds up to a total of 120 ml during the experiment. As seen in Figure 40 the air bubble reaches an approximate final size of 5 x 3 x 2 cm (l x w x h). The area directly above the transducer, at the bottom of the cavity is very brittle and easily breaks upon a slight tap with a screw driver. The inside wall of the cavity seems to be well rounded and very smooth. This can be interpreted as an effect of tiny cavitation bubbles that dissolve the ice at the water interface.

Figure 40: Block of ice after 20 minutes of ultrasonic excitation. A cavity as an effect of ultrasonic cavitation is seen.

In a control experiment the ice filled, frozen ultrasonic cleaner is left without any ultrasonic excitation at room temperature. After 40 minutes only 10 ml of water are removed from the tank. This leads to the insight, that the disintegration under ultrasonic excitation is 24 times faster. Even in comparison to the least successful US experiment, which dissolved 60 ml after 20 minutes, the non-ultrasonic disintegration is 12 times slower.

## 4.2 Setup 2 – Duration of ice plug dissolution

The control experiment shows, that leaving the ice-filled, frozen steel cylinder with an initial temperature of -18°C untouched for eight hours at a room temperature of 22°C, 260 ml of ice melts. Extrapolated to the total volume of 3000 ml it would take 92.3 hours to melt. The ice plug inside is removed after the experiment. It shows a regular smooth surface in form of a cylinder as it is expected when ice melts under normal conditions.

The experiments under ultrasonic excitation show a much faster disintegration of the ice plug inside the cylinder. Although, three tests with different ultrasonic energy outputs are performed realized with 2, 4 or 10 transducers operating, no significant differences in dissolution time and ice shape are noticeable. Therefore, the intermediate test with 4 transducers and 400 W power output is presented in this thesis. The total excitation time is 160 minutes. The average resonant frequency is 26.11 kHz and has tendency to decrease with time. This makes sense as ice melts and ultrasonic waves get dissipated faster in a liquid medium compared to a hard ice block. The signal amplitude stays constant at 1.4 A. The temperature profile can be seen in Figure 41.

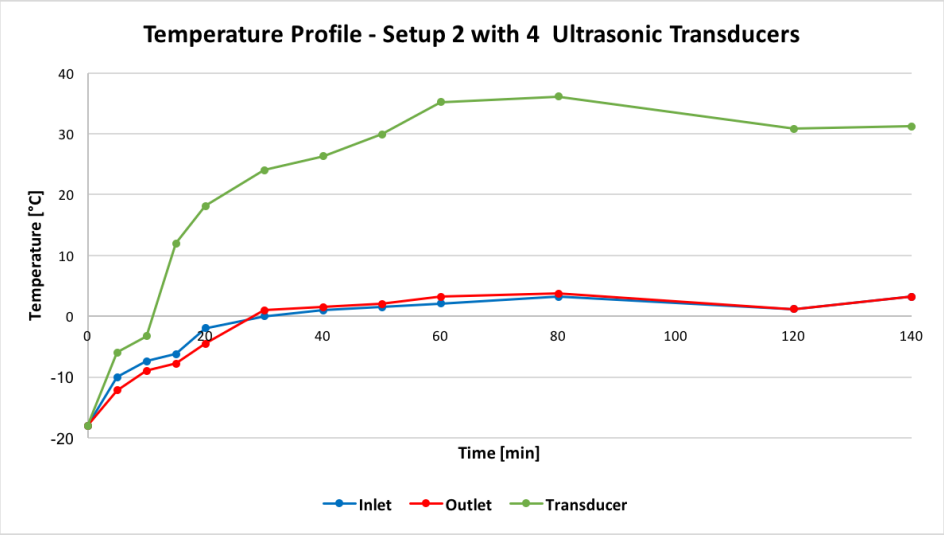


Figure 41: Temperature profile of Setup 2 with 4 ultrasonic transducers operating (400 W)

After 140 minutes of excitation the ultrasonic signal is terminated to visually check the appearance of the ice plug. Significant changes and differences compared to the non-ultrasound test are visible. The surface of the ice is severely attacked by the ultrasonic signal and is extremely brittle. The ice is disintegrated and dissolved in blocky breakouts and shows deep holes, fractures and a rough surface (Figure 42). The ice is put back in and additionally treated for 20 minutes. During this time, the disintegration was even faster as it is shown in Figure 43. In the end only two pieces of a compacted inner core is left.

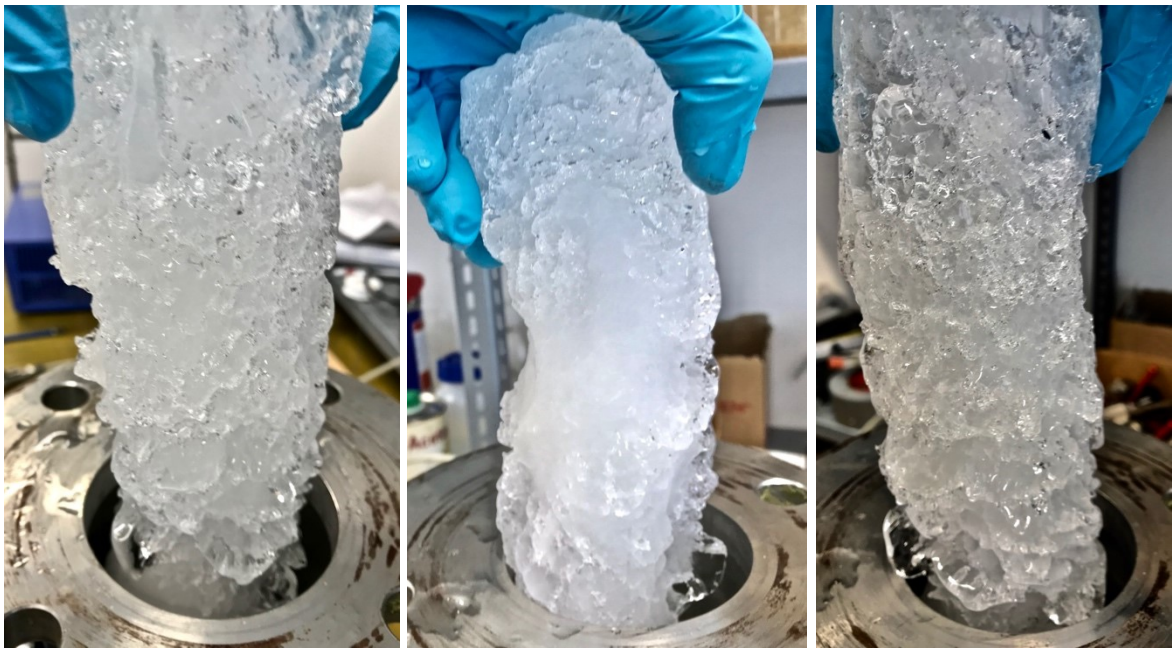

Figure 42: Block of ice after 140 minutes of US treatment showing a very rough surface.

Figure 43: Remaining inner ice core after 160 minutes of ultrasonic excitation.

After the total treatment time of 160 minutes the remaining ice is removed and molten volume is measured. It adds up to 2710 ml of water which nearly is the total volume of the cylinder. Proving that the disintegration of ice with the help of ultrasound is a powerful technique. Extrapolating this result to the total of 3000 ml it would take approximately 3 hours to melt the entire ice. In direct comparison to the non-ultrasound treatment with 92.3 hours it is about 30 times faster.

## 4.3 Setup 3 – Pressure breakthrough time of a plugged steel cylinder

As mentioned earlier Setup 3 conducts the breakthrough time of a high pressure which is applied at the inlet of the steel cylinder. This breakthrough time is a crucial parameter as it clarifies at which point a pressure or flow communication between inlet and outlet is granted. Therefore, represents the time how long it takes until a plugged pipe can flow again. Figure 44 shows a comparison of a pressure profiles with and without ultrasonic excitation. The upper chart, the non-ultrasound experiment (NonUS_4), states a breakpoint (BP) after 37 minutes and 26 seconds. The BP of the ultrasonic treatment (US_2; 2 transducers) comparatively occurs after 12 minutes and 34 seconds. This is an overall improvement of about 300 %. In addition to the BP the molten volume after 50 minutes, which marked the end of the experiment, is surveyed. After the experiment NonUS_4 850 ml water can be removed. In comparison, 1460 ml are measured after experiment US_2, which is an increase of about 70 %.

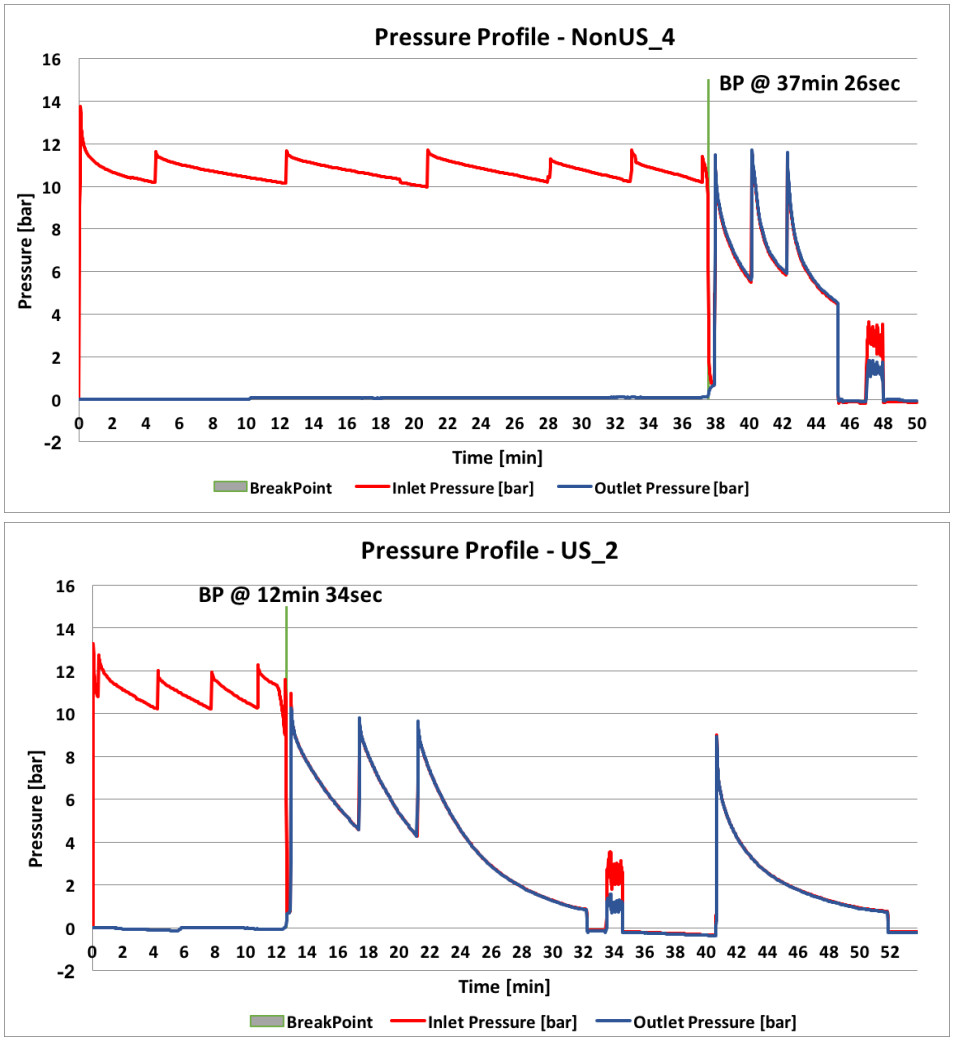


Figure 44: Pressure profiles of experiments NonUS_4 and US_2 showing a clear difference in breakthrough points.

Comparing the temperature profile of the non-ultrasound and the ultrasound experiment, a clear increase of temperature of the steel cylinder is determined under ultrasonic excitation (Figure 45). At the beginning, they are quite the same but after 25 minutes both inlet and outlet temperature of US_2 are in the range of 5°C whereas in NonUS_4 they are around 0°C. Maximum temperature reaches 10.3°C in US_2 and 3.2°C in NonUS_4. Leading to the assumption that the generated heat during the transformation from an electrical signal to the mechanical ultrasonic vibration inside of the transducers has a relevant effect on faster disintegration times under ultrasonic excitation. Which severity this impact has, could be an evaluation for further scientific studies and is not discussed in this thesis.

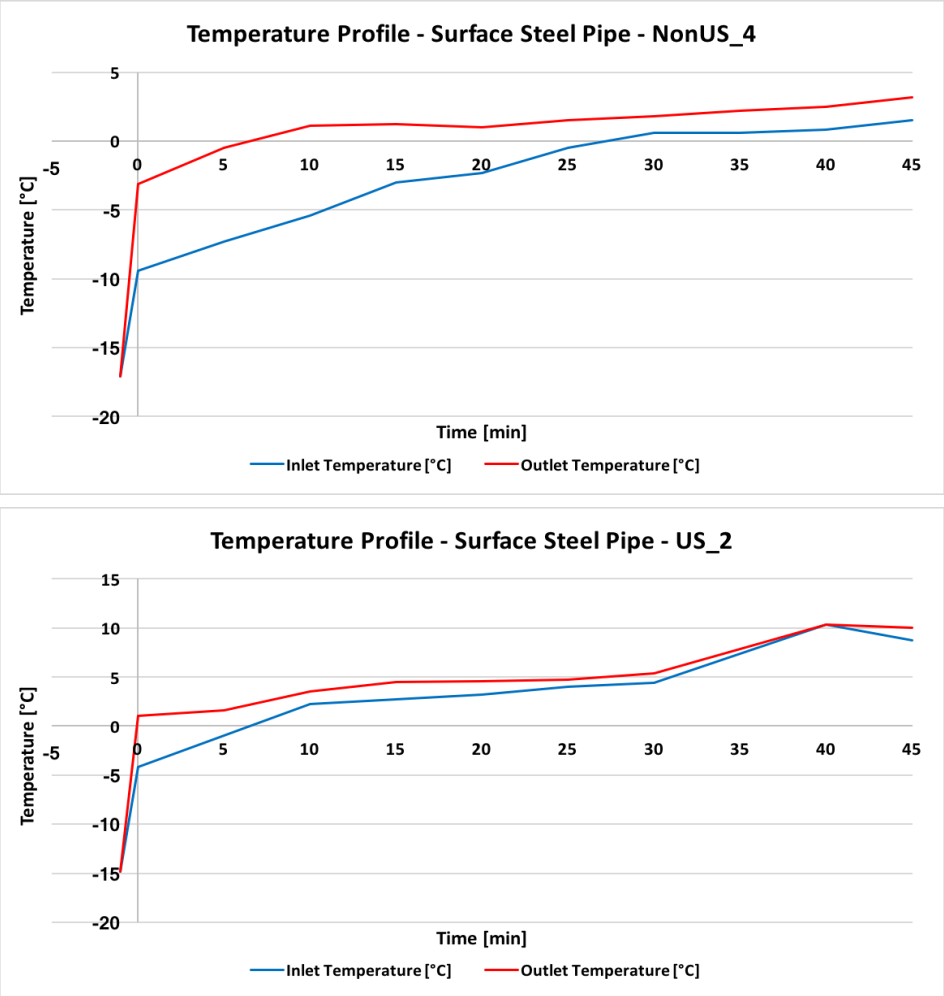


Figure 45: Temperature Profiles of experiments NonUS_4 and US_2 showing an elevated pipe temperature during ultrasonic excitation.

Another evaluation to possibly see an enhancement due to ultrasonic treatment is the calculation of internal flow resistance. Therefore, all valves are opened after the BP is reached and a circulation through the cylinder is simulated by pumping water continuously

for one minute. The average pressure difference between inlet and outlet is calculated and interpreted as the resistance to free flow inside the cylinder due to the block of ice. But as seen in Figure 46 the comparison of both experiments doesn't indicate any difference. Delta p comparing NonUS_4 and US_2 is 1.44 bar and 1.43 bar, respectively. Coming to realization that once the breakthrough is reached the pressure finds its way through the ice, no matter if it is disintegrated with the help of US or not.

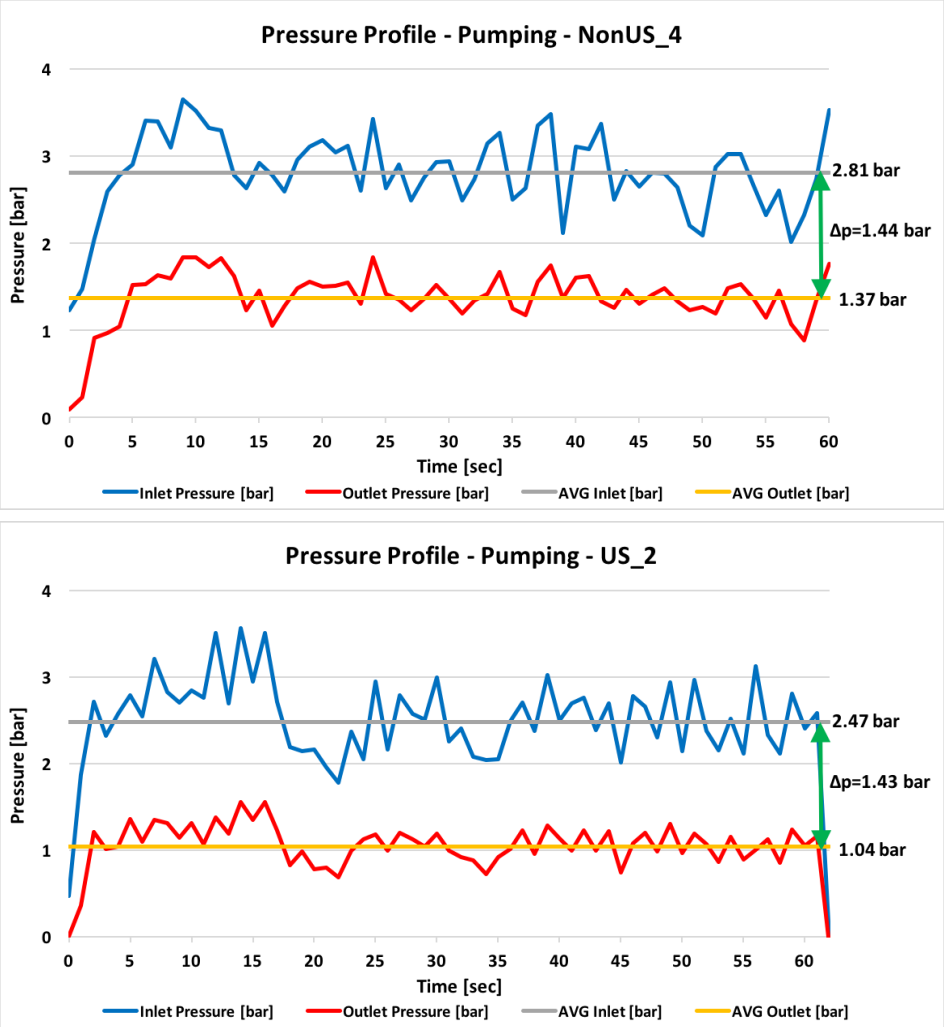


Figure 46: Pumping pressure profiles to determine average inlet and outlet pressure to get an idea about internal flow resistance.

A comprehensive overview of results of all performed experiments with Setup 3 are presented in Table 12. Generally, experiments NonUS_4 and US_2 are chosen to be compared as they represent the results of all conducted experiments most accurately.

Table 12: Summary of results from experimental Setup 3.

| | NonUS_1 | NonUS_2 | NonUS_3 | NonUS_4 | NonUS_5 | US_1 | US_2 | US_3 | US_4 | US_5 | US_6 |
|---|---|---|---|---|---|---|---|---|---|---|---|
| *Fozen Volume [ml]* | | | | | | 3000 | | | | | |
| *Time in Freezer [hr]* | | | | | | > 24 | | | | | |
| *Initial Pressure [bar]* | 11,10 | 14,60 | 13,00 | 13,60 | 14,56 | 12,13 | 13,26 | 13,61 | 13,21 | 14,32 | 13,67 |
| *Break Point [mm:ss]* | 38:44 | 32:47 | 22:50 | 37:26 | 25:41 | 12:03 | 12:34 | 23:52 | 14:40 | 16:03 | 14:11 |
| *Pressure Equal [mm:ss]* | 41:17 | 35:43 | 23:43 | 37:51 | 27:33 | 12:26 | 12:54 | 25:01 | 15:01 | 16:15 | 14:22 |
| *Open Valves [mm:ss]* | 60:36 | 41:33 | 25:47 | 45:26 | 35:01 | 41:24 | 32:13 | 30:12 | 30:00 | 30:32 | 30:29 |
| *Pumping Time [sec]* | 60 | 51 | 60 | 60 | 61 | 40 | 62 | 60 | 60 | 61 | 60 |
| *Pumped Volume [ml]* | 1450 | 1740 | 2150 | 2240 | 2230 | 1600 | 2240 | 2400 | 2270 | 2300 | 2300 |
| *Pump Rate [l/h]* | 87,0 | 122,8 | 129,0 | 134,4 | 131,6 | 144,0 | 130,1 | 144,0 | 136,2 | 135,7 | 138,0 |
| *Average Inlet Pressure [bar]* | - | 1,81 | 2,1 | 2,81 | 2,87 | 2,32 | 2,47 | 2,79 | 2,53 | 2,65 | 2,60 |
| *Average Outlet Pressure [bar]* | - | 0,94 | 0,93 | 1,37 | 1,55 | 0,99 | 1,04 | 1,24 | 1,13 | 1,05 | 1,09 |
| *Delta P [bar]* | - | 0,87 | 1,17 | 1,44 | 1,32 | 1,33 | 1,43 | 1,55 | 1,40 | 1,60 | 1,51 |
| *End of Experiment [mm:ss]* | 65:00 | 50:00 | 30:00 | 50:00 | 50:00 | 50:00 | 50:00 | 50:00 | 50:00 | 50:00 | 50:00 |
| *Molten Volume [ml]* | - | 800 | 620 | 850 | 840 | 1410 | 1460 | 1220 | 1300 | 2020 | 2100 |
| *Maximum Inlet Temperature [°C]* | - | 1,5 | 1,6 | 1,5 | 1,6 | 7,5 | 8,7 | 5,6 | 6,1 | 7,4 | 8,1 |
| *Minimum Outlet Temperature [°C]* | - | 2,8 | 2,9 | 3,2 | 2,9 | 11,1 | 10 | 6,2 | 8,1 | 6,5 | 7,4 |
| *Maximum Transducer Temperature [°C]* | - | - | - | - | - | 45,1 | 80,5 | 35,2 | 41,7 | 60,0 | |
| *Number of Transducers* | - | - | - | - | - | 2 | 2 | 4 | 4 | 10 | 10 |
| *Power Input [W]* | - | - | - | - | - | 200 | 200 | 400 | 400 | 1000 | 1000 |
| *Average Resonant Frequency [kHz]* | - | - | - | - | - | 24,8 | 24,9 | 23,3 | 23,4 | 23,5 | 23,6 |
| *Average Signal Amplitude [A]* | - | - | - | - | - | 1,72 | 1,78 | 1,56 | 1,54 | 1,75 | 1,80 |

# 5 Conclusion / Recommendations

This thesis discusses the influence of ultrasonic waves on ice under different conditions and setups. Main influencing parameters such as,

- treatment duration
- ultrasonic energy input and
- pressure

are determined. Parameters including

- ice disintegration time
- pressure breakthrough time
- molten volume
- delta p
- resonant frequency
- wave amplitude
- inlet/outlet temperature and
- transducer temperature

are evaluated and compared. A clear improvement of ice disintegration time under ultrasound is seen throughout all experiments (Figure 47). Generally, the dissolution is faster with increasing treatment duration. Under pressure the disintegration of the ice plug was more effective as under ambient conditions. Variations of ultrasonic energy input up to 400 W are ineffective as no significant changes are noticeable. A substantial improvement is reached at 1000 W, as the total disintegration of 3000 ml of ice is twice as fast (Figure 48).

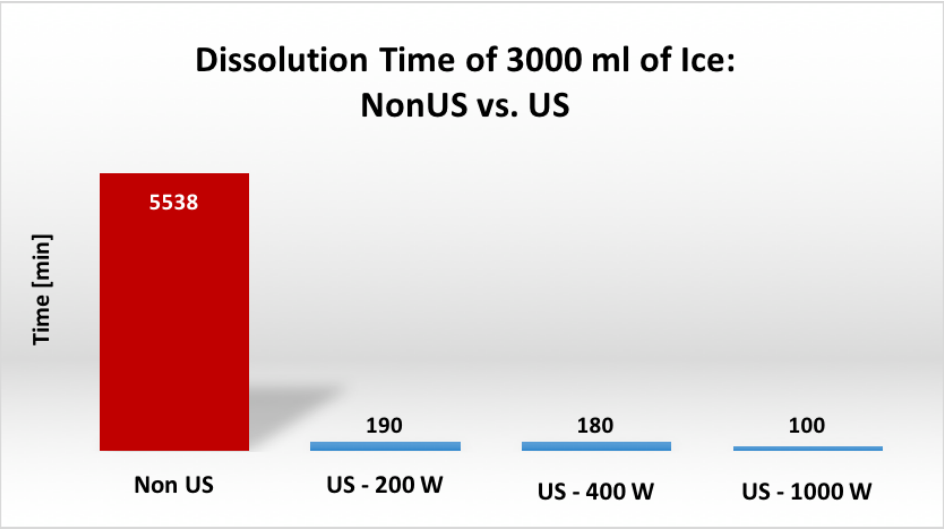


Figure 47: Comparison of ice dissolution times between non-ultrasonic and ultrasonic treatment.

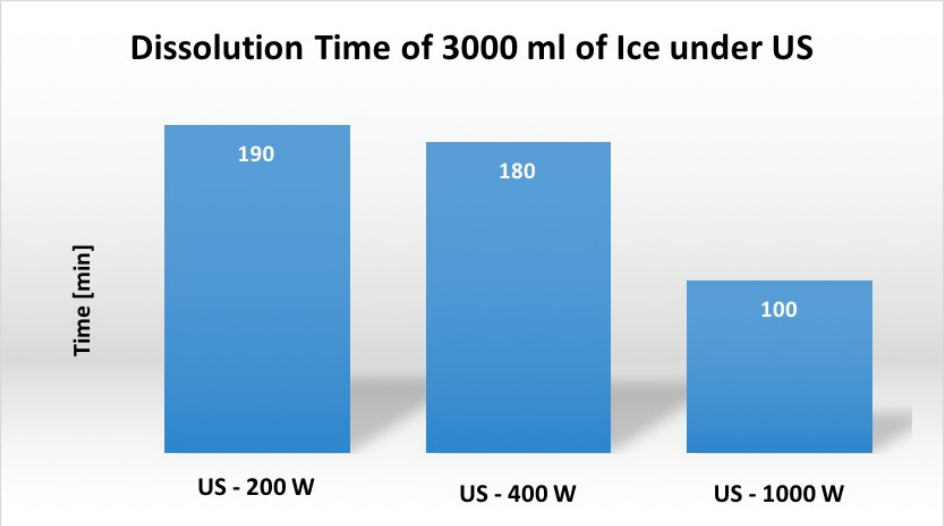


Figure 48: Comparison of ice dissolution times between different ultrasonic energy inputs.

Pressure breakthrough times are basically independent of treatment duration and ultrasonic energy input. Although, an approximately two times faster breakthrough is achieved under ultrasonic excitation in direct contrast to non-sonicated experiments (Figure 49). Different pressure regimes are not tested in particular, but logical assumptions indicate that an increase in pressure will lead to shorter breakthrough times.

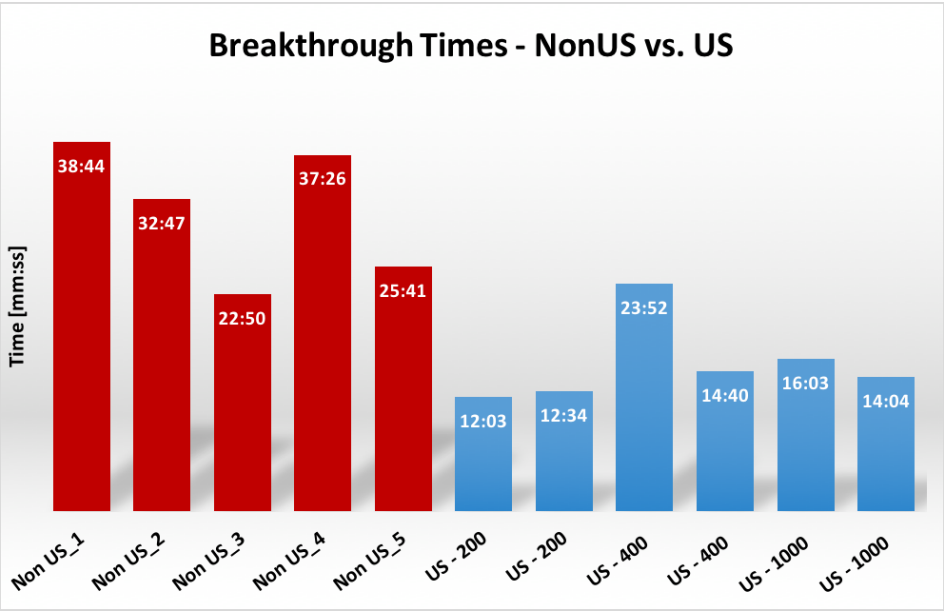


Figure 49: Pressure breakthrough times: (red) no ultrasonic treatment; (blue) with ultrasonic treatment. A clear decrease in breakthrough times is visible.

The observed trend seen in Figure 49 can also be noticed when comparing molten volumes after the ultrasonic excitation. An increase of volume with factors between 1.4 and 3.4 are evaluated (Figure 50).

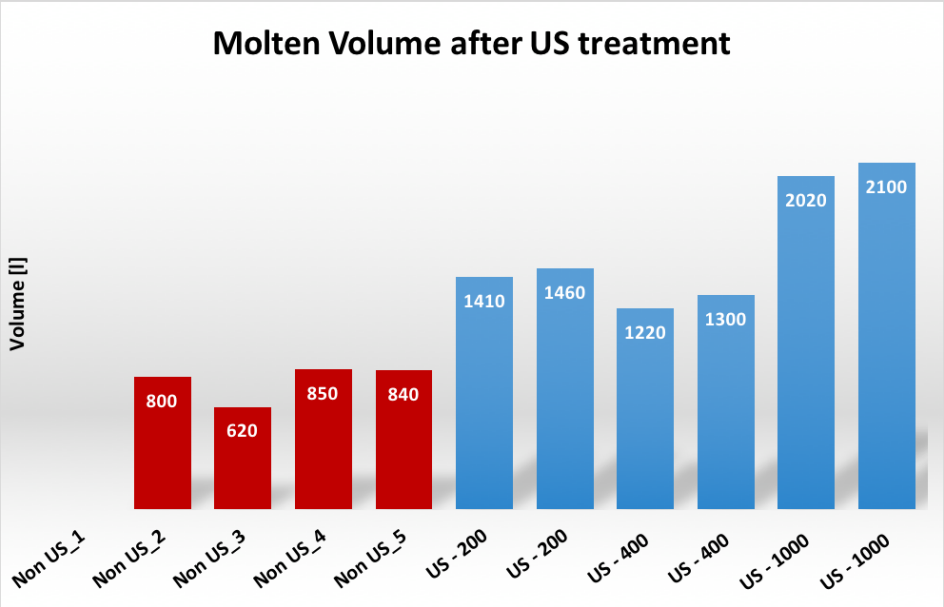


Figure 50: Comparison of molten volume at the end of the experiment.

Delta p, representing the resistance to free flow inside the pipe, stays roughly the same and shows no improvement due to the ultrasound treatment (Figure 51). The pressure drop between inlet and outlet is probably governed by the shape of the steel cylinder and is maybe different in another setup.

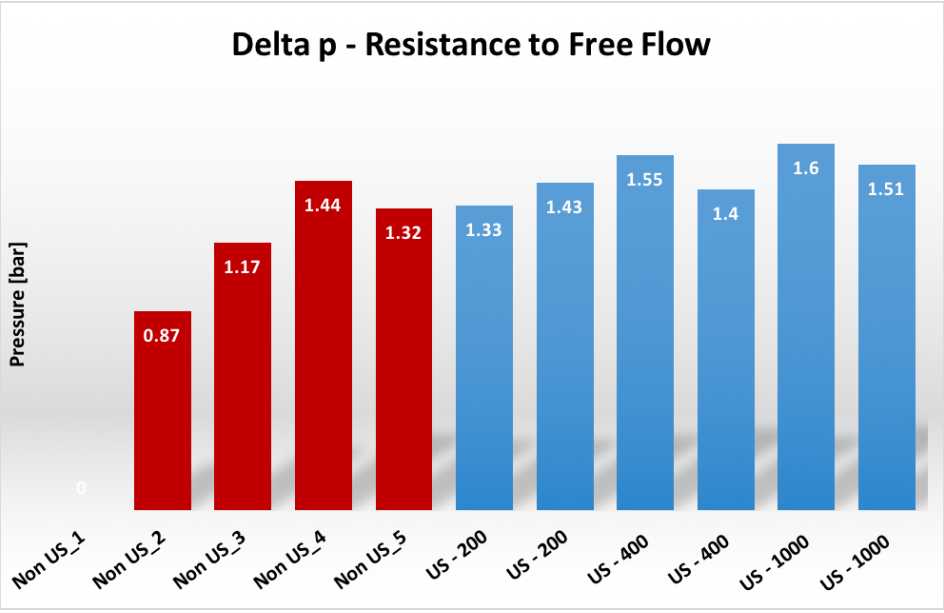


Figure 51: Comparison of delta p – resistance to free flow.

As seen in Figure 52 ultrasound has a major effect on inlet and outlet temperature at the surface of the steel cylinder. This is explained on the one hand due to the ultrasonic energy dissipation of the steel wall as well as of the ice inside the cylinder. And on the other hand, due to the heat generation inside the ultrasonic transducer during the transformation from an electrical signal to the mechanical ultrasonic vibration. It is assumed that these elevated temperature lead to a faster dissolution of the ice plug. For further clarification experiments under isolated conditions need to be performed.

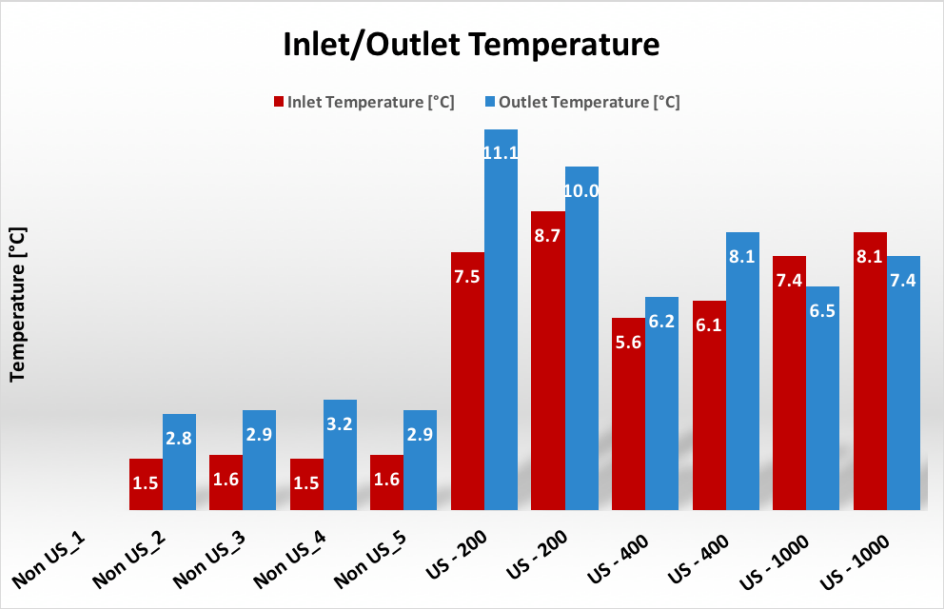


Figure 52: Comparison of Inlet/Outlet temperature at the surface of the steel cylinder.

In summary, the overall objective of this thesis is fulfilled as a clear impact of ultrasound on ice as a substitute for natural gas hydrates is observed. It therefore, could represent a new remediation method for hydrate plugs. To further validate its feasibility additional research should be performed. Recommendations for future experiments are:

- Comparison of ultrasonic remediation to conventional removal methods
- Experiments under isolated temperature conditions
- Experiments under constant fluid flow
- Evaluation of the effect of different ultrasonic frequencies
- Applying ultrasound on actual natural gas hydrates in the field

# 6 References

[1] M. Amro, M. Al-Mobarky and E. Al-Homadhi, "Improved Oil Recovery by Application of Ultrasound Waves to Waterflooding," in *15th SPE Middle East Oil & Gas Show and Conference*, Bahrain, 2007.

[2] D. Sloan, C. A. Koh and A. K. Sum, Natural Gas Hydrates in Flow Assurance, Houston, Pau, Golden: Elsevier, 2011.

[3] J. Carol, Natural Gas Hydrates 3rd Edition, Calgary: Gulf Professional Publishing is an imprint of Elsevier, 2014.

[4] S. Caicedo, "Feasability Study of Ultrasound for Oilwell Stimulation Based on Wave Properties Consideration," in *SPE Latin American and Caribbean Petroleum Engineering Conference*, Buenos Aires, 2007.

[5] F. Van der Bas and e. al., "Radial Near Wellbore Stimulation by Acoustic Waves," in *SPE International Symposium and Exhibition on Formation Damage Control* , Lafayette, 2004.

[6] T. Wu, N. Guo, C. Teh and J. Hay, "Theory and Fundamentals of Ultrasound," in *Advances in Ultrasound Technology for Environmental Remediation*, Springer, Dordrecht, 2013.

[7] J. Fuchs, "Ultrasonic Cleaning: Fundamental Theory and Application," Blackstone NEY Ultrasonics, Jamestown, NY, 2002.

[8] F. Gaitan and e. al., "Sonoluminescence and bubble dynamics for a single, stable, cavitation bubble," *Journal Acoustical Society America,* vol. 91, no. 6, pp. 3166-3183, 1992.

[9] J. Keller and M. Miksis, "Bubble oscillations of large amplitudes," *Acoustical Society America ,* vol. 68, no. 2, 1980.

[10] A. Prosperetti and L. Crum, "Nonlinear bubble dynamics," *Acoustical Society America,* vol. 82, no. 2, 1987.

[11] H. G. Flynn, "Cavitation dynamics. I. A mathematical formulation," *Acoustical Society America,* vol. 57, no. 6, 1975.

[12] R. D. Duhon and J. M. Campbell, "The Effect of Ultrasonic Energy on the Flow of Fluids in Porous Media," in *Second Anual Eastern Regional Meeting of the Society of*

*Petroleum Engineers*, Charleston, 1965.

[13] I. A. Beresnev and P. A. Johnson, "Elastic-wave stimulation of oil production: A review of methods and results," *Geophysics,* vol. 59, no. 6, pp. 1000-1017, 1994.

[14] M. Akhmetov, M. Muduev and A. Abdulaev, "Application of acoustic method for preventing salts precipitation: Oil Industry," no. 9, pp. 13-14, 1977.

[15] M. Mullakaev, V. Abramov and A.V.Abramova, "Development of ultrasonic equipmen tand technology for well stimulation and enhanced oil recovery," *Journal of Petroleum Science and Engineering,* no. 125, January 2015.

[16] K. Jeehyeong and N. Seungmin, "Ultrasonic Effects on Water Flow Through Porous Media," *International Journal of Offshore and Polar Engineering,* vol. 16, no. 2, pp. 146-152, 2006.

[17] N. A. Noruddin and W. Sulaiman, "Macro-Model and Micro-Model Observation on The Effect of Intermittent," *Australian Journal of Basic and Applied Sciences,* pp. 324-332, September 2016.

[18] T. Hamida and T. Babadagli, "Effect of Ultrasonic Waves on the Capillary-Imbibition Recovery of Oil," in *Asia Pacific Oil & Gas Conference and Exhibition*, Jakarta, 2005.

[19] T. Hamida and T. Babadagli, "Capillary Interaction of Different Oleic and Aqueous Phases Between Matrix and Fracture Under Ultrasonic Waves," in *SPE Europec/EAGE Annual Conference*, Madrid, 2005.

[20] T. Hamida and T. Babadagli, "Effects of Ultrasonic Waves on Immiscible and Miscible Displacement in Porous Media," in *2005 SPE Technical Conference and Exhibition*, Dallas, Texas, 2005.

[21] T. Hamida and T. Babadagli, "Investigations on Capillary and Viscous Displacement Under Ultrasonic Waves," *Journal of Canadian Petroleum Technology,* vol. 45, no. 2, pp. 16-19, 2006.

[22] M. Cil, J. Reis, M. Miller and D. Misra, "An Examination of Countercurrent Capillary Imbibition Recovery from Single Matrix Blocks and Recovery Predictions by Analytical Matrix/Fracture Transfer Functions," in *SPE Annual Technical Conference and Exhibition*, New Orleans, 1998.

[23] P. Poesio, G. Ooms and F. Van der Bas, "An investigation of the influence of acoustic waves on the liquid flow through a porous material," *Journal Acoustical Society America,* vol. 111, no. 5, pp. 2019-2025, 2002.

[24] A. Aarts, G. Ooms, K. Bil and E. Bot, "Enhancement of Liquid Flow Through a Porous Medium by Ultrasonic Radiation," in *SPE European Petroleum Conference*, The Hague, 1998.

[25] G. Xiao, "1.1 High Frequency Vibration Recovery Enhancement Technology in the Heavy Oil Fields of China," in *SPE International Thermal Operations and Heavy Oil Symposium and Western Regional Meeting*, Bakersfield, 2004.

[26] E. Mohammadian, "Enhancing Oil Recovery through Application of Ultrasonic Assisted Waterflooding," in *SPE Asia Pacific Oil and Gas Conference and Exhibition*, Jakarta, 2011.

[27] A. Venkitaraman and P. Roberts, "Ultrasonic Removal of Near-Wellbore Damage Caused by Fines and Mud Solids," in *SPE Formalion Damage Symposium*, Lafayette, LA, 1994.

[28] P. Roberts, "Ultrasonic Removal of Organic Deposits and Polymer Induced Formation Damage," in *SPE Formation Damage Control Symposium*, Lafayette, Louisiana, 1996.

[29] S. B. Awad, "Ultrasonic Cavitations and Precision Cleaning," *Precision Cleaning - The Magazine of Critical Cleaning Technology,* pp. 12-17, 1996.

[30] S. Shedid, "An ultrasonic irradiation technique for treatment of asphaltene deposition," *Journal of Petroleum Science and Engineering,* vol. 42, pp. 57-70, 2004.

[31] H. Hofstaetter and M. Pavlov, "Application of Ultrasound for the Destruction of Resin-Paraffin Deposits in Pipeline Transport of Oil," Ufa, 2014.

[32] B. Champion, F. Van der Bas and G. Nitters, "The Application of High-Power Sound Waves for Wellbore Cleaning," in *SPE European Formation Damage Conference*, The Hague, 2003.

[33] S.-W. Wong, W. Van der Bas and P. Zuiderwijk, "High Power/High Frequency Acoustic Stimulation - A Novel and Effective Wellbore Stimulation Technology," in *SPE Annual Technical Conference and Exhibition*, Denver, 2003.

[34] F. Van der Bas, E. Rouffignac and P. Zuiderwijk, "Acoustic Stimulation to Mitigate Near-Wellbore Damage," in *SPE Annual Technical Conference and Exhibition*, Houston, 2004.

[35] H. Kunanz and S. Wölfel, "Scale Removal with Ultrasonic Waves," in *SPE International Oilfield Scale Conference and Exhibition*, Aberdeen, 2014.

[36] H. Hamidi, E. Mohammadian and R. Rafati, "The Effect of Ultrasonic Waves on Oil

Viscosity," Taylor & Francis Group, LLC, Kuala Lumpur, 2014.

[37] M. Amani, A. Retnanto, S. AlJuhani and e. al., "Investigating the Role of Ultrasonic Wave Technology as an Asphaltene Flocculation Inhibitor, an Experimental Study," in *2015 International Petroleum Technology Conference*, Doha, 2015.

[38] A. A. Tagiltcev and V. I. Korenbaum, "The Effect of Ultrasonic Oscillations of Pipe on Fluidity of Heavy Oil Products," in *ISOPE Pacific/Asia Offshore Mechanics Symposium*, 2012.

[39] T. Chen, R. Chow, J.-Y. Yuan and A. Babchin, "A Physical Preventive Treatment of Crystallization and Precipitation in the Petroleum Industry," in *Petroleum Society's Canadian International Petroleum Conference*, Calgary, 2001.

[40] B. F. Towler, A. K. Chejara and S. Mokhatab, "Experimental Investigations of Ultrasonic Waves Effects on Wax Deposition During Crude-Oil Production," in *2007 SPE Annual Technical Conference and Exhibition*, Anaheim, 2007.

[41] M. Maslin, O. Mathew and B. Richard, "Gas hydrates: past and future geohazard?," *Philosophical Transactions of the Royal Society,* vol. 368, no. 1, pp. 2369-2393, 2010.

[42] Wikipedia, "Wikipedia - the free encyclopedia," [Online]. Available: https://en.wikipedia.org/wiki/Methanol_toxicity. [Accessed 12 September 2018].

[43] Wikipedia, "Wikipedia - the free encyclopedia," [Online]. Available: https://en.wikipedia.org/wiki/Ethylene_glycol_poisoning. [Accessed 12 September 2018].

[44] Y. P. Handa and C. J. G., "Thermal Conductivity of Xenon Hydrate," *The Journal of Physical Chemistry,* vol. 91, no. 25, pp. 6327-6328, December 1987.

[45] Y. F. Makogon, Hydrates of Hydrocarbons, Texas: Penn Well Books, 1997.

[46] J. H. Keenan, Steam Tables: Thermodynamic Properties of Water Including Vapor, Liquid, and Solid Phases, New York: John Wiley & Sons, 1978.

[47] D. E. Sloan and C. A. Koh, Clathrate Hydrates of Natural Gases, Third Edition, Boca Raton: CRC Press, 2007.

[48] GT-Sonic, "gtsonic.net," GT Sonic, [Online]. Available: https://www.gtsonic.net/prod_view.aspx?TypeId=91&id=268&fid=t3:91:3. [Accessed 3 September 2018].

[49] UCE-Ultrasonic, "ultra-piezo.com," UCE Ultrasonic, [Online]. Available: http://www.ultra-piezo.com/Products/ultrasonic-transducer/ultasonic-cleaning-tansducer/1.html.

[Accessed 3 September 2018].

[50] UCE-Ultrasonic, "ultra-piezo.com," UCE Ultrasonic, [Online]. Available: http://www.ultra-piezo.com/Products/ultrasonic-generator/ultrasonic-cleaning-generator/74.html. [Accessed 3 September 2018].

[51] Testo, "testo.com," Testo, [Online]. Available: https://www.testo.com/en/testo-549-i/p/0560-1549. [Accessed 3 September 2018].

# Appendices

## Appendix A

Electric scheme of the ultrasonic generator UCE-NT2500.

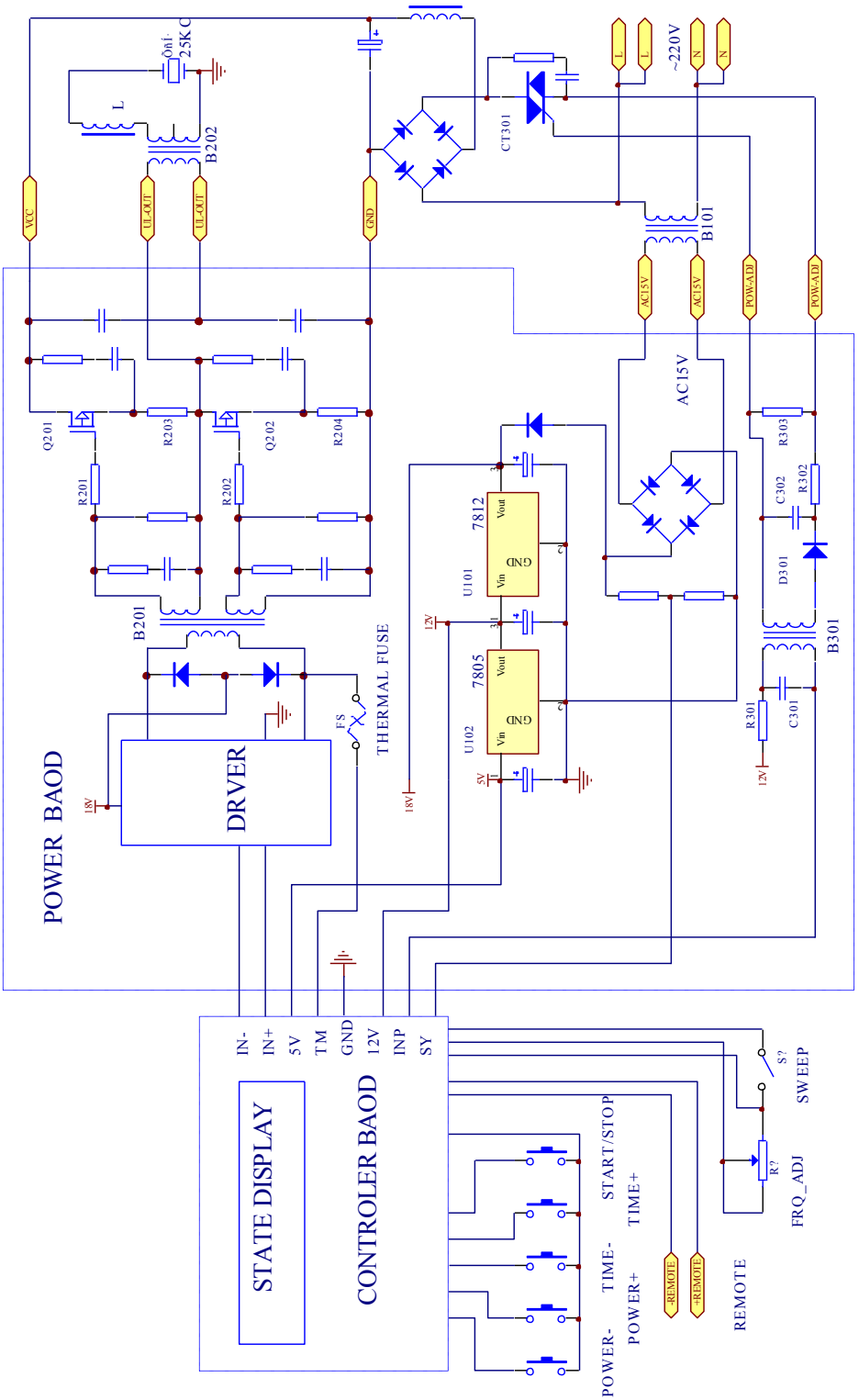

# Appendix B

Graphical representation of the main setup of the laboratory experiment.